Recent studies of heavy ion transfer reactions using large solid angle magnetic spectrometers

Suzana Szilner
Ruđer Bošković Institute, Zagreb
PRISMA collaboration

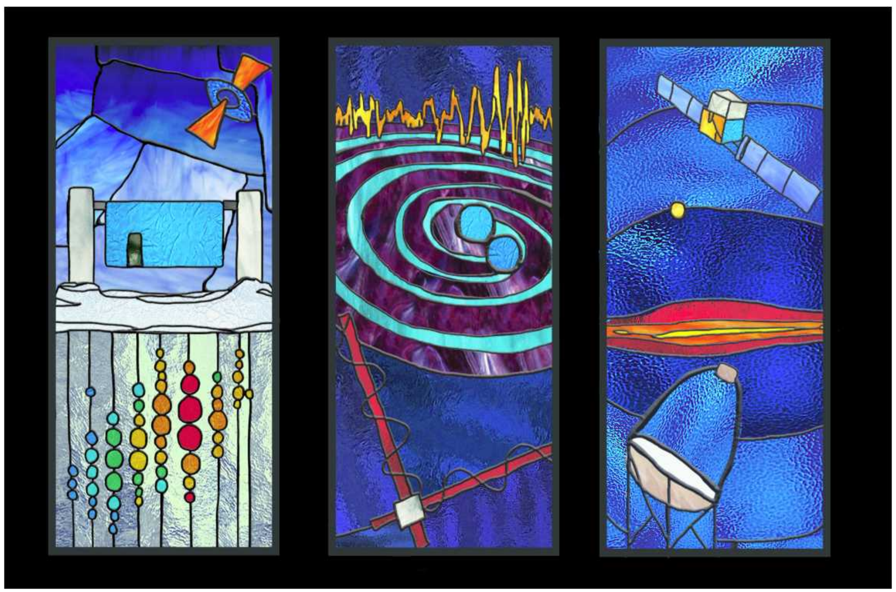

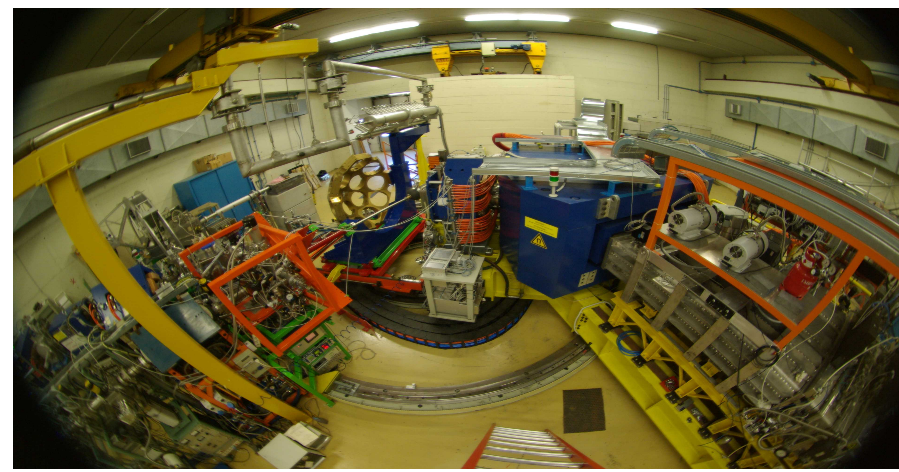

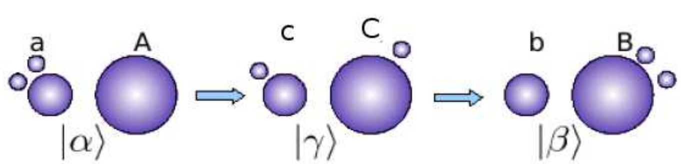

NSD 2019
NSD2019
13-17 May, 2019 - Venice, Italy
Centro culturale Don Orione Artigianelli

Heavy ion transfer reactions

neutron rich nuclei

heavy nuclei

synthesis in lab

correlations → nucleon - nucleon → studies of pairing in nuclei

correlations → mass – mass → instrumental: coincident detection of partners → studies of production of heavy neutron-rich nuclei

reaction mechanism → above the barrier

reaction mechanism → below the barrier

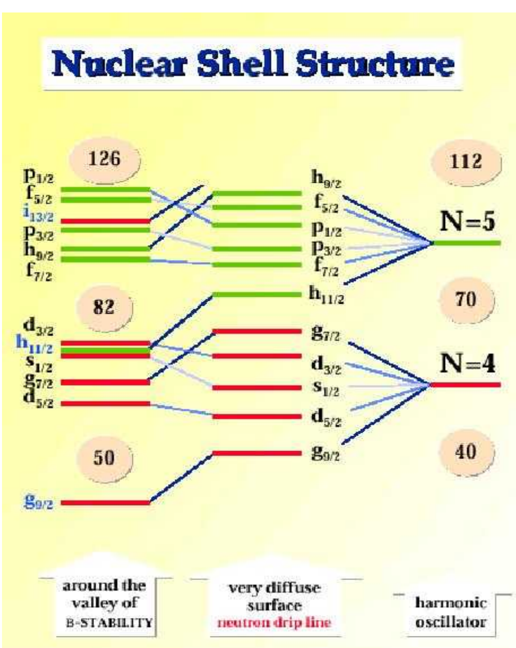

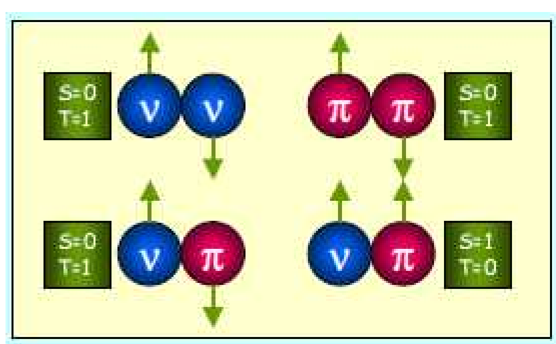

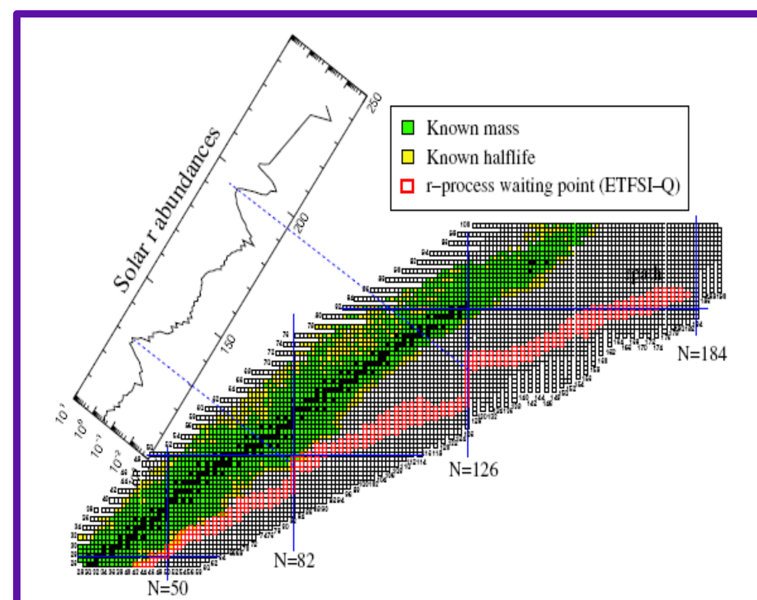

Probing nucleon-nucleon correlations in transfer reactions

The pairing interaction induces particle-particle correlations that are essential in defining the properties of finite quantum many body systems in their ground and neighboring states. These structure properties may influence in a significant way the evolution of the collision of two nuclei.

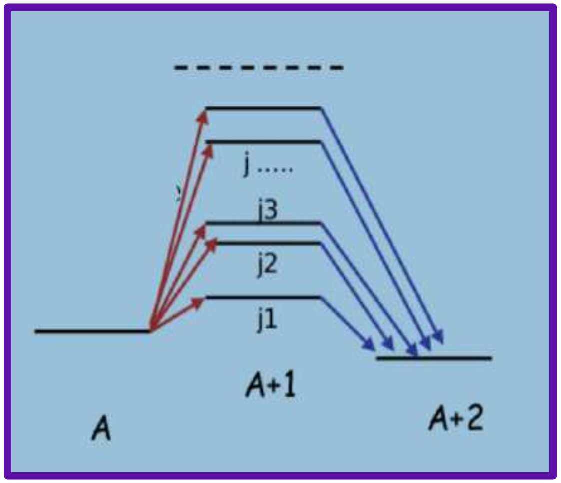

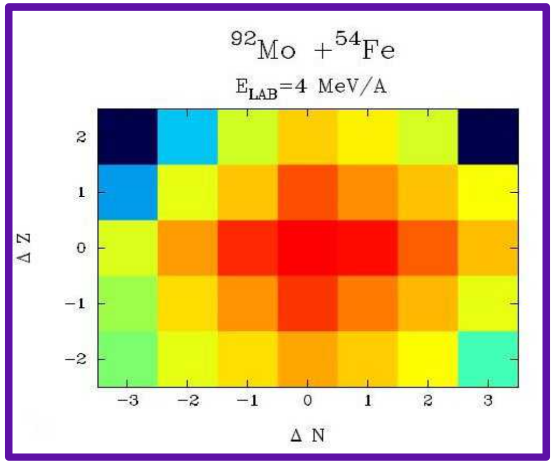

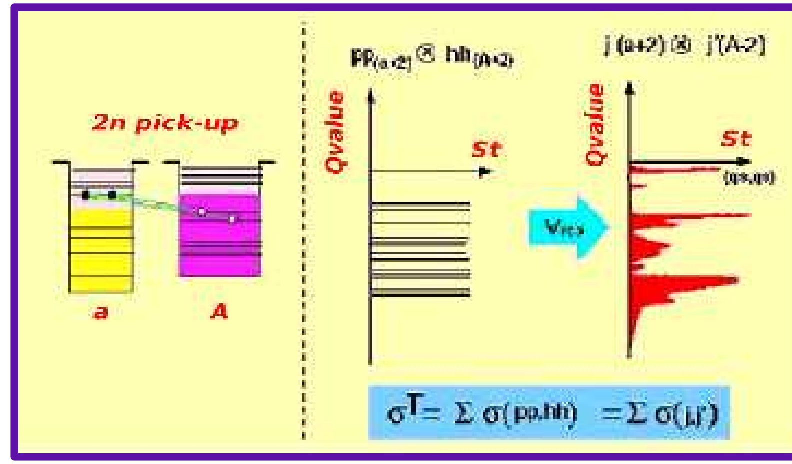

Heavy ion transfer reactions:

Advantages: test of correlation properties in transfer processes via simultaneous comparison of ±n and ±p, and ±nn/±pp/±np pairs; transfer of "many" pairs
HI drawbacks: limited A,Z, energy resolutions (two-nucleon transfer → redistribution of the strength around single particle states)

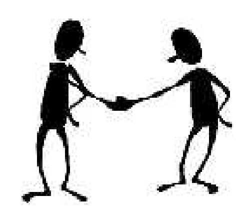

Absolute cross sections for one and two-nucleon transfer reactions

$^{208}Pb(^{16}O,^{18}O_{g.s.})^{206}Pb$

______ successive+simultaneous

- - - - - -simultaneous

Theoretical treatment: the structure information is entangled with the reaction mechanism (complex structure of the two interacting ions, QE and DIC processes, many open channels).

full quantum-mechanical

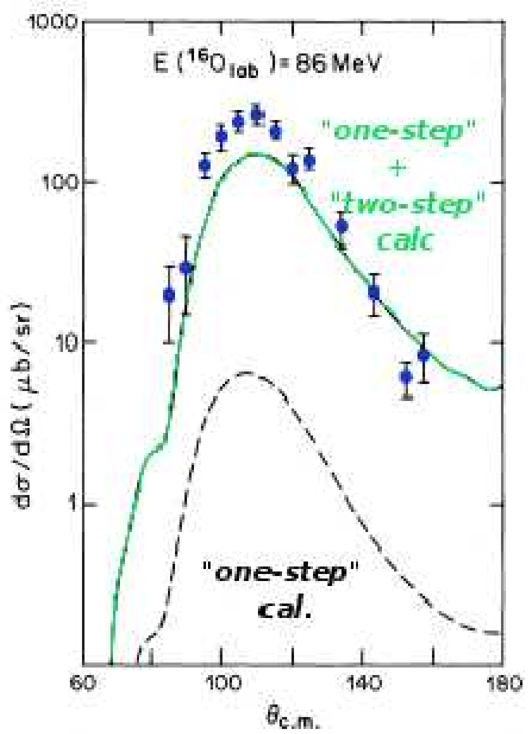

B.F.Bayman and J.Chen, Phys. Rev. C 26 (1982) 1509

semi-classical

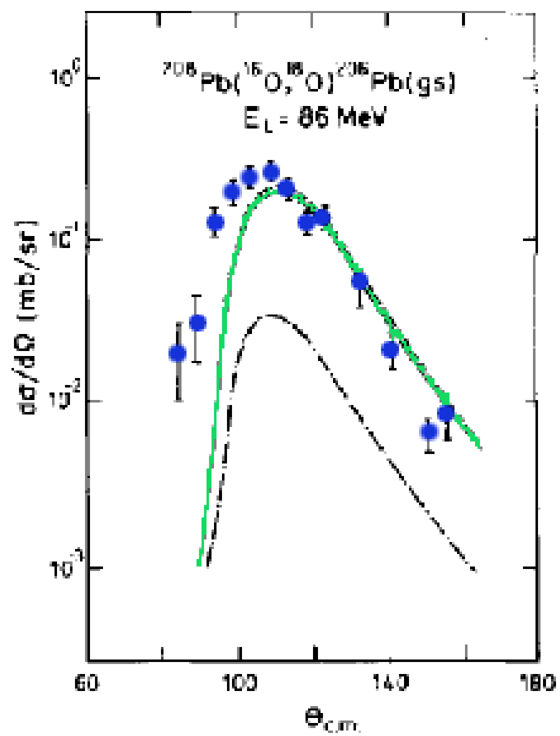

E.Maglione, G.Pollarolo, A.Vitturi, R.A.Broglia and A.Winther Phys. Lett. B 162 (1985) 59

full quantum-mechanical

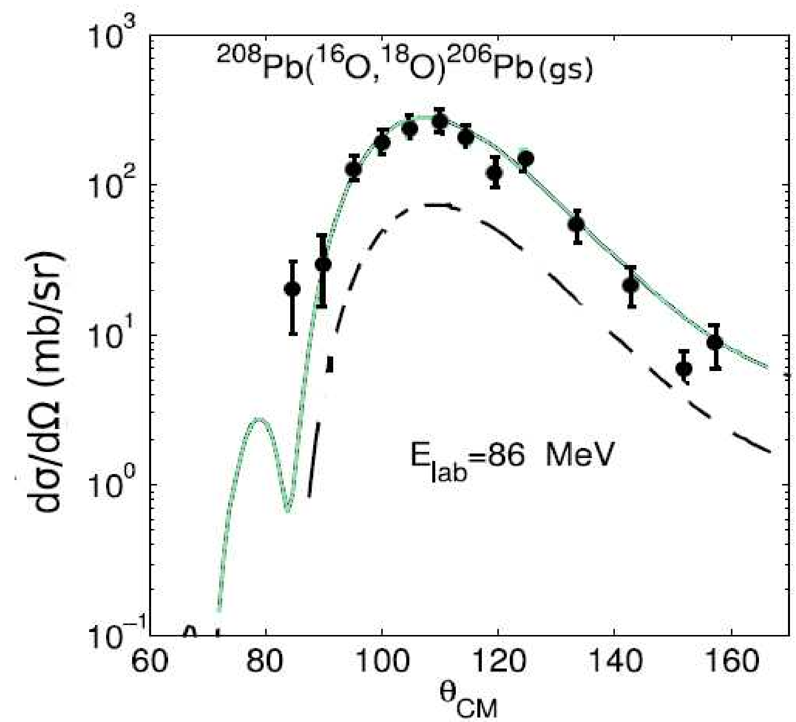

G.Potel, A.Idini, F.Barranco, E.Vigezzi and R.A.Broglia, Rep. Prog. Phys. 76 (2013) 106301;

G. Potel et al, PRL 105 (2010) 172502

Absolute cross sections for one and two-nucleon transfer reactions

$^{208}Pb(^{16}O,^{18}O_{g.s.})^{206}Pb$

______successive+simultaneous

- - - - - -simultaneous

microscopic theories: include correlations + the coupling between relative motion (reaction) + intrinsic motion (structure).

full quantum-mechanical

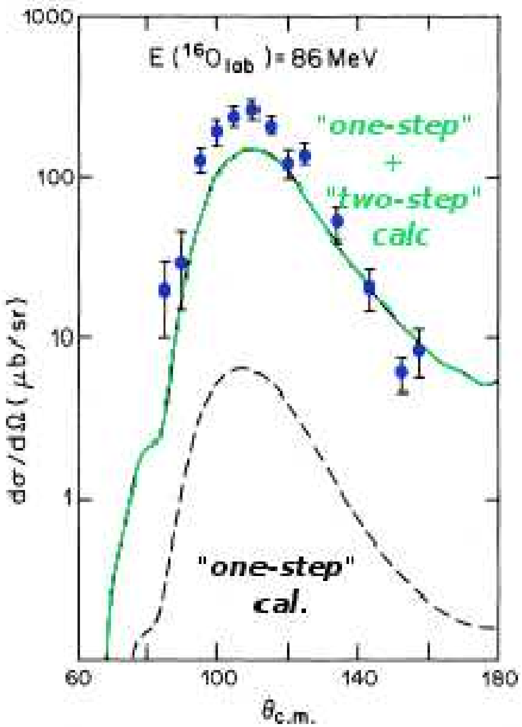

B.F.Bayman and J.Chen, Phys. Rev. C 26 (1982) 1509

semi-classical

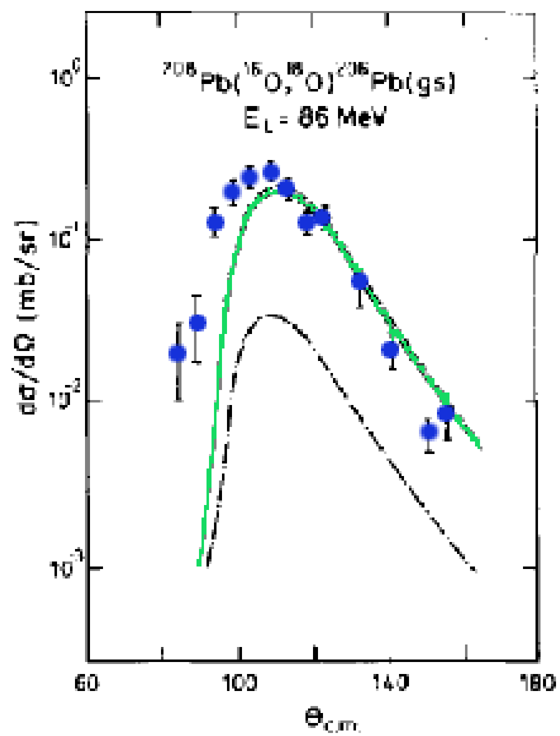

E.Maglione, G.Pollarolo, A.Vitturi, R.A.Broglia and A.Winther Phys. Lett. B 162 (1985) 59

full quantum-mechanical

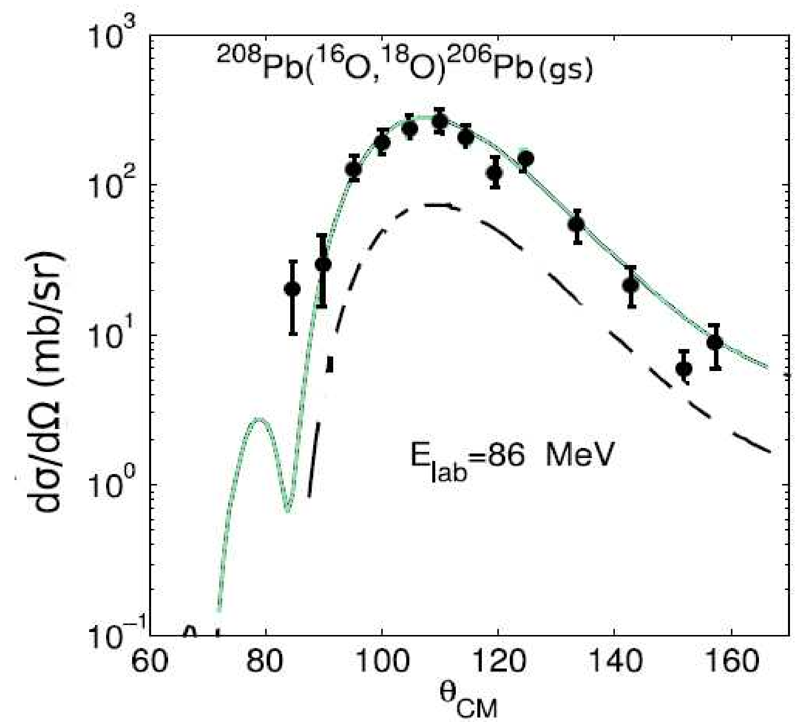

G.Potel, A.Idini, F.Barranco, E.Vigezzi and R.A.Broglia, Rep. Prog. Phys. 76 (2013) 106301;

G. Potel et al, PRL 105 (2010) 172502

Magnetic spectrometer PRISMA

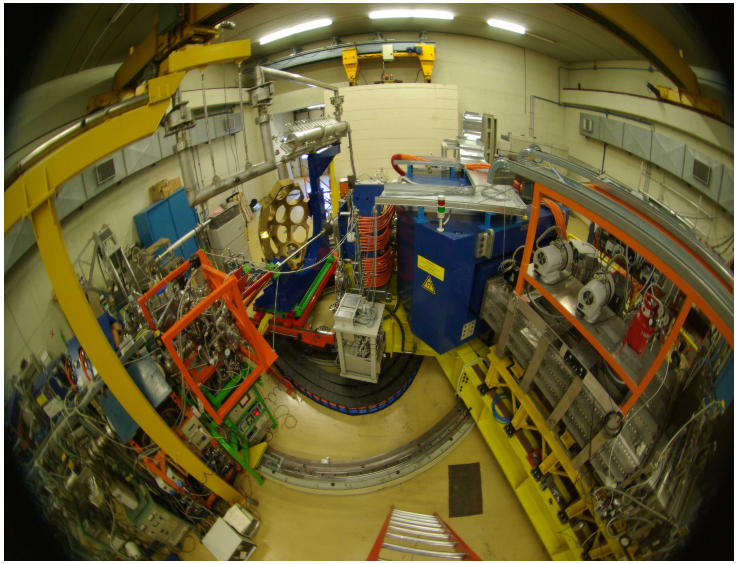

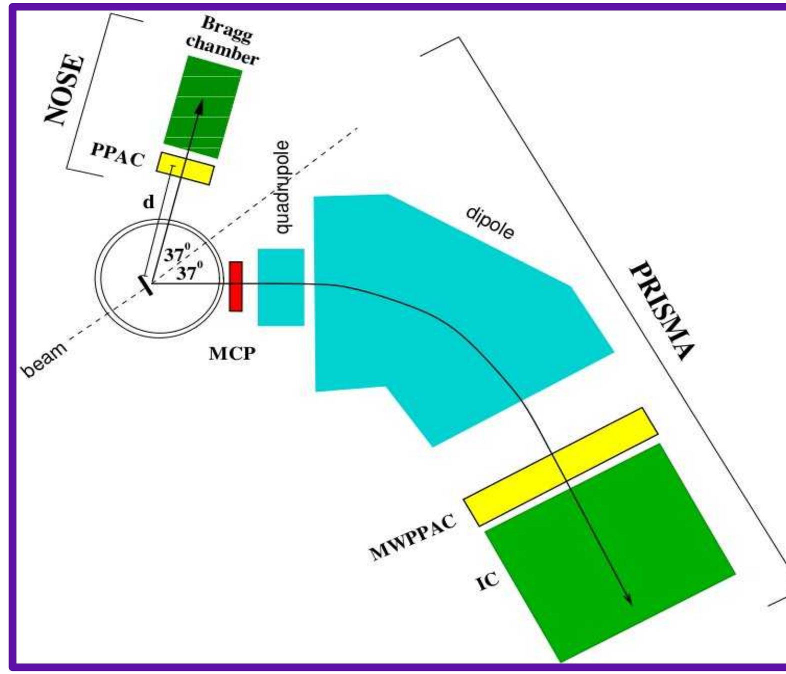

magnets: quadrupole + dipole
detectors:
start detector: MCP – micro-channel plate
focal plane detectors: MWPPAC – multiwire parallel plate avalanche counter, IC – ionization chamber

PRISMA:
$\Omega \approx 80$ msr $B\rho_{max} = 1.2$ Tm
$\Delta A/A \sim 1/200$
$\Delta Z/Z \sim 1/60$ for $Z=20$
E acceptance $\approx \pm 20\%$

position in MCP: X_i, Y_i
focal plane position: x_f, y_f
Time of Flight: $ToF = t_f - t_i$
energy loss, total energy: ΔE, E - IC

→ **event-by-event trajectory reconstruction** →

A, q, Z, E, v
mass, charge, atomic state, energy, velocity

$^{40}Ar+^{208}Pb$, $^{40}Ca+^{208}Pb$, and $^{58}Ni+^{208}Pb$

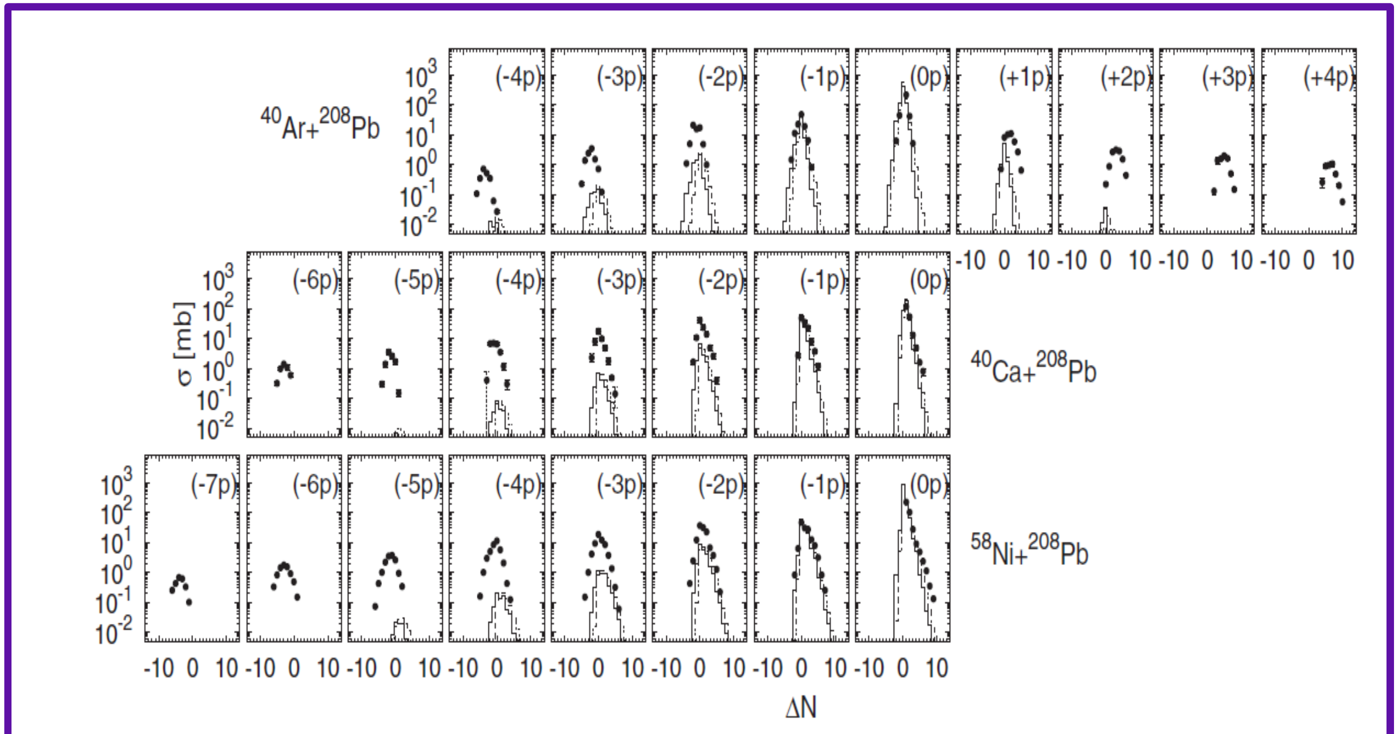

Above the barrier:
→ many open channels, transfer of 5-10 protons and neutrons governed by optimum Q-value
→ large TKEL, onset of DIC components
→ secondary processes: evaporation, transfer induced fission

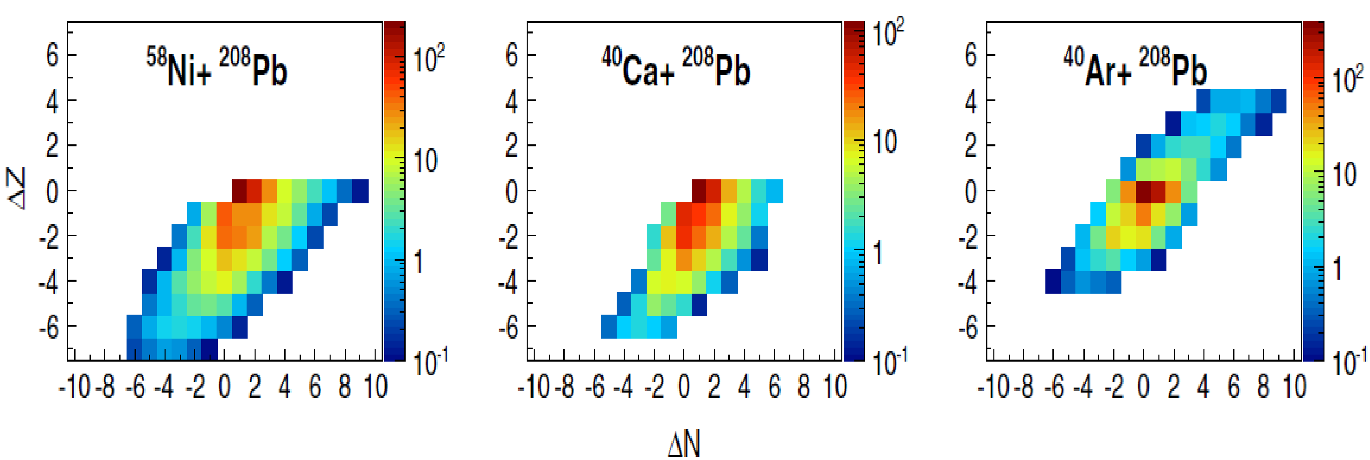

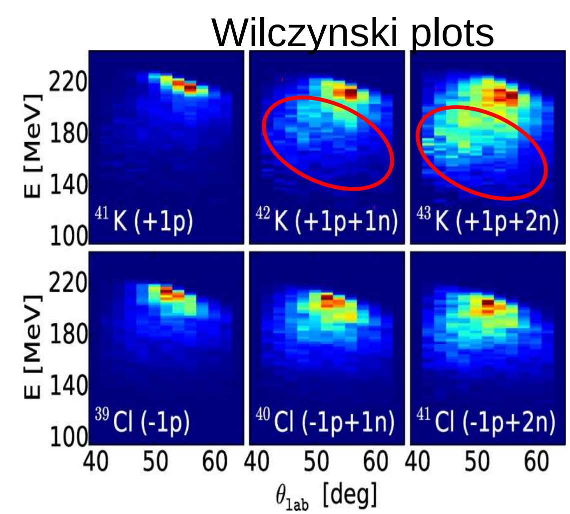

$^{40}Ar+^{208}Pb$

T. Mijatovic et al., Phys. Rev. C 94 (2016) 064616

Multinucleon transfer reactions : experiment vs. theory

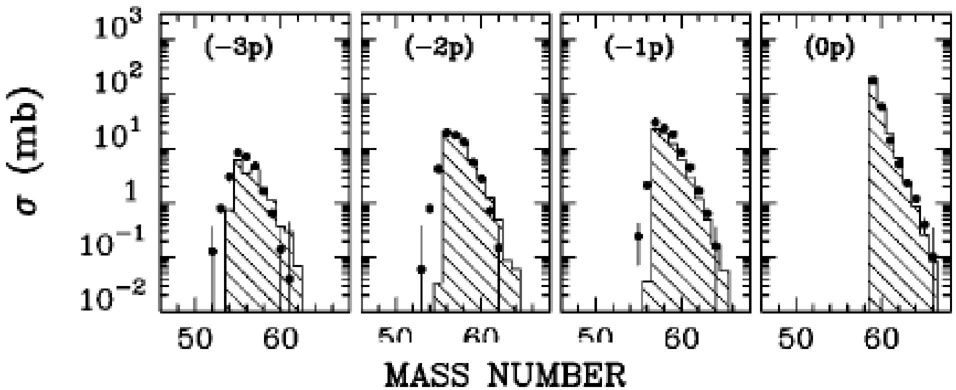

^{58}Ni+^{208}Pb, L. Corradi et al., PRC 66 (2002) 024606 (GRAZING or CWKB, G. Pollarolo)

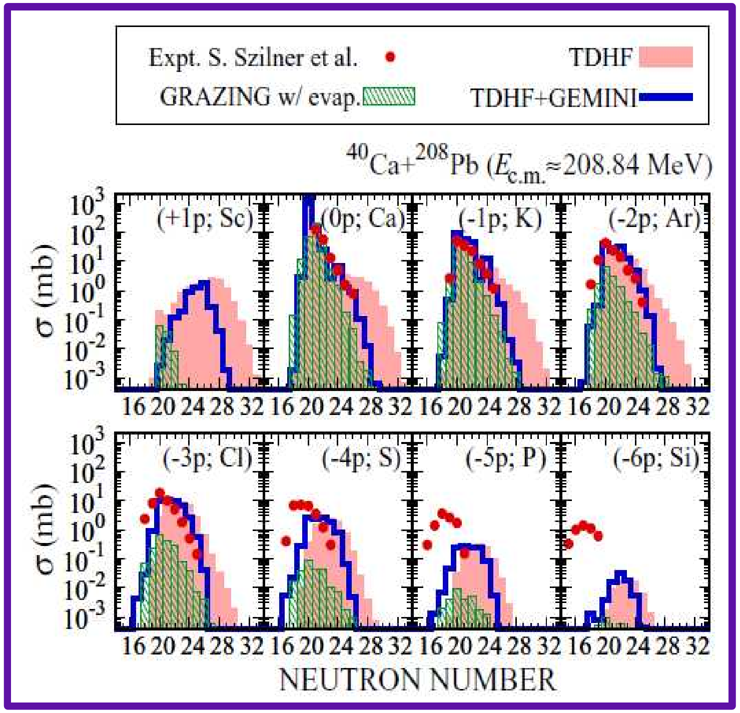

Time Dependent Hartree-Fock theory
K.Sekizawa, K.Yabana, PRC 88 (2013) 014614
K.Sekizawa PRC 96 (2017) 014615
C. Simenel, A.S. Umar, Progress in Part. and Nucl. Phys. 103 (2018) 19

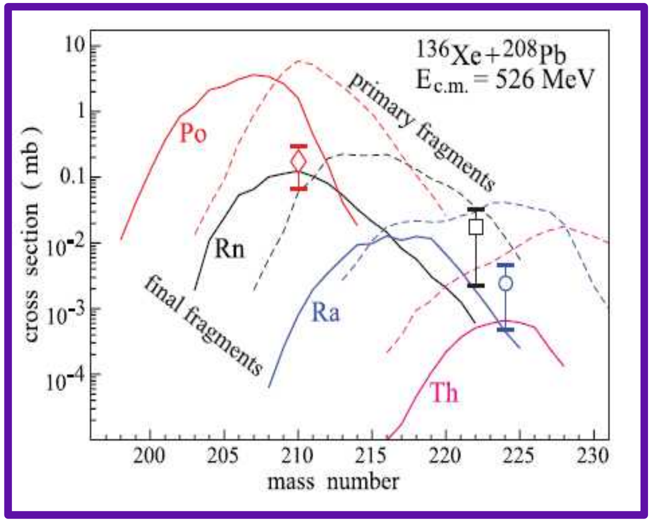

Langevin-type approach
V. Zagrebaev, W. Greiner PRL 101 (2008) 122701; PRC 83 (2011) 044618
A.V.Karpov and V.V.Saiko, PRC 96 (2017) 024618

W. Sargsyan et al., PRC 88 (2013) 064601
K. Hagino and G. Scamps, PRC 92 (2015) 064602
QMD: Long Zhu et al., PLB 791 (2019) 20
….

Nucleon-nucleon correlations studied with PRISMA

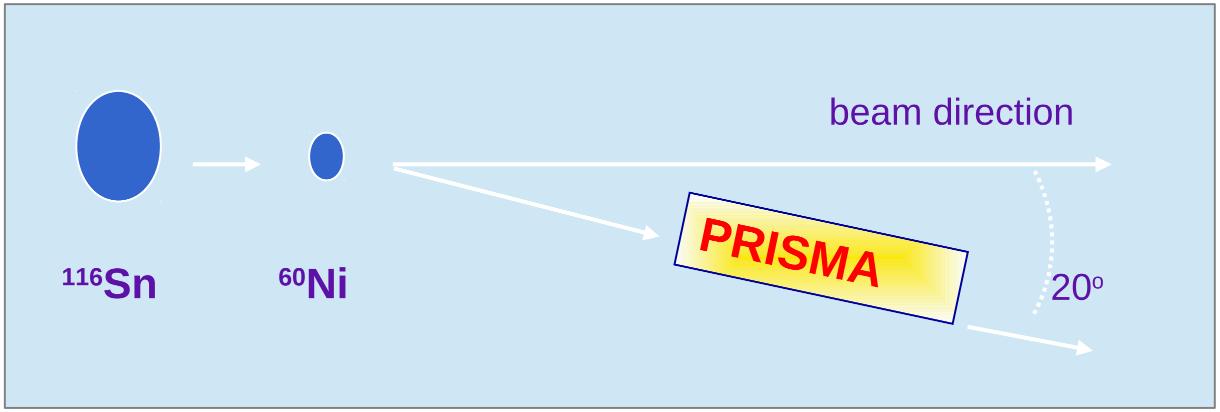

$^{116}Sn+^{60}Ni$, inverse kinematic, excitation function (detection of (lighter) target-like fragment in PRISMA:

E_{beam} = 500 MeV – 410 MeV

(D ~ 12.3 to 15.0 fm)

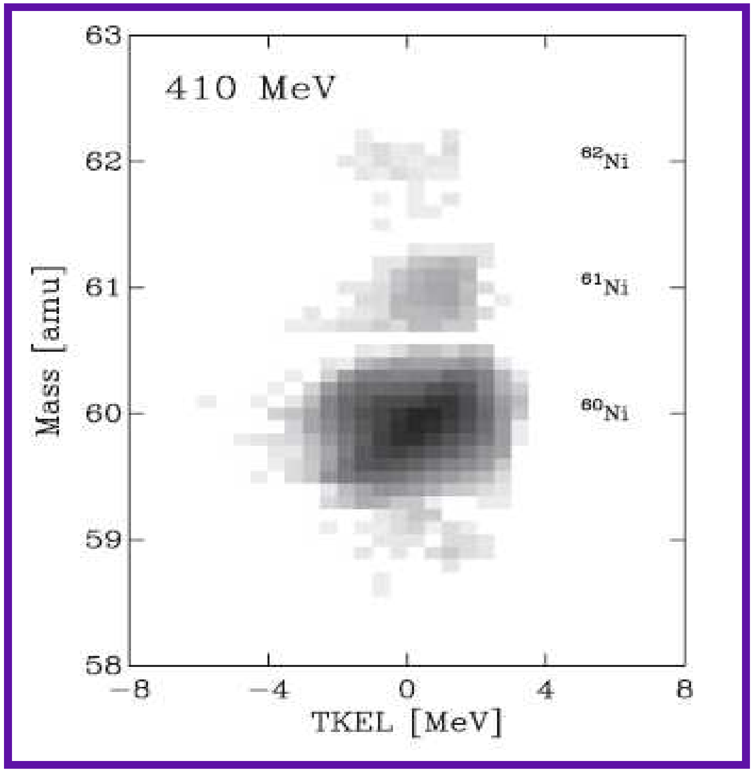

$^{96}Zr+^{40}Ca$, $^{116}Sn+^{60}Ni$, $^{92}Mo+^{54}Fe$, $^{206}Pb+^{116}Sn$
direct + inverse kinematic (7 experiments)

$^{96}Zr+^{40}Ca$: S. Szilner et al., Phys. Rev. C 76 (2007) 024604; L. Corradi et al., Phys. Rev. C 84 (2011) 034603
$^{116}Sn+^{60}Ni$: D. Montanari et al., Phys. Rev. Lett. 113 (2014) 052501; D. Montanari et al., Phys. Rev. C 93 (2016) 054623
$^{92}Mo+^{54}Fe$: T. Mijatovic talk, Multinucleon transfer reactions and proton transfer channels, TUE, Sala Goldoni, 15:20

Measurements below Coulomb barrier

$^{116}Sn(^{60}Ni,^{62}Ni)$
$Q_{gs} = +1.3$ MeV

A smooth transition between QE and DIC

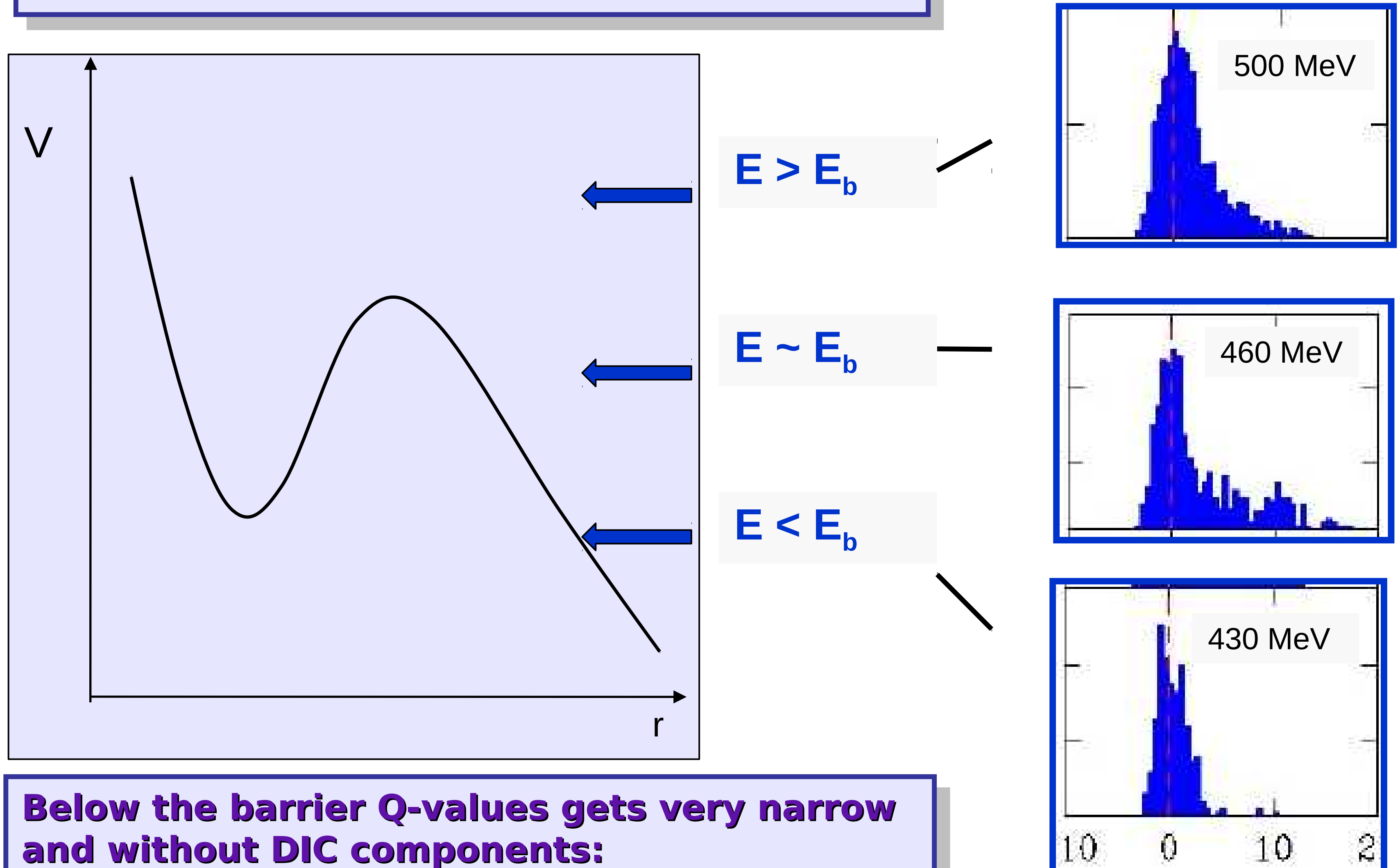

Below the barrier Q-values gets very narrow and without DIC components:
1) $E > E_b$ large number of open channels, DIC components / evaporation effects
2) $E < E_b$ narrow Q-value distributions (concentrated at "one state")

D. Montanari et. al., PRL 113 (2014) 052501

$^{116}Sn+^{60}Ni$: neutron pair transfer far below the Coulomb barrier

Transfer strength very close to the g.s. to g.s. transitions

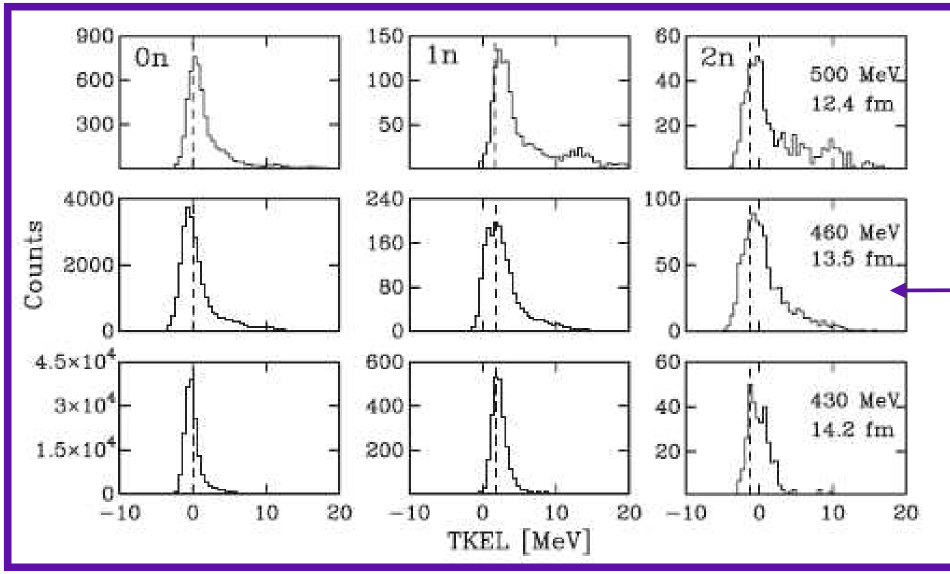

D. Montanari et. al., Phys. Rev. Lett. 113 (2014) 052501

Coulomb barrier

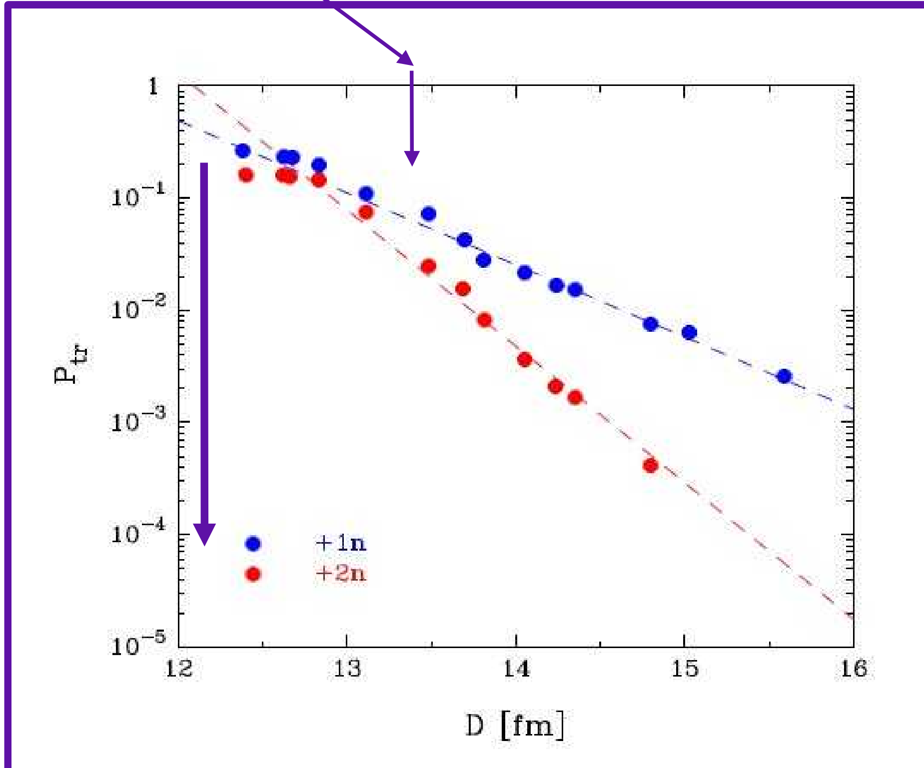

$$P_{tr} = \frac{d\sigma_{tr}}{d\sigma_{\mathrm{Ruth}}}$$

$$D = \frac{Z_a Z_A e^2}{2E_{\mathrm{c.m.}}}\left(1 + \frac{1}{\sin(\theta_{\mathrm{c.m.}}/2)}\right)$$

^{60}Ni+^{116}Sn, ^{40}Ca+^{96}Zr, ^{54}Fe+^{92}Mo: fragment – gamma measurements (PRISMA+CLARA/AGATA/LaBr)

^{60}Ni+^{116}Sn: angular distributions measurement in "direct" kinematic:

E_{beam} = 245 MeV at 70^0 (D ~ 14.5 fm)

$$D = \frac{Z_a Z_A e^2}{2E_{\mathrm{c.m.}}}\left(1 + \frac{1}{\sin(\theta_{\mathrm{c.m.}}/2)}\right)$$

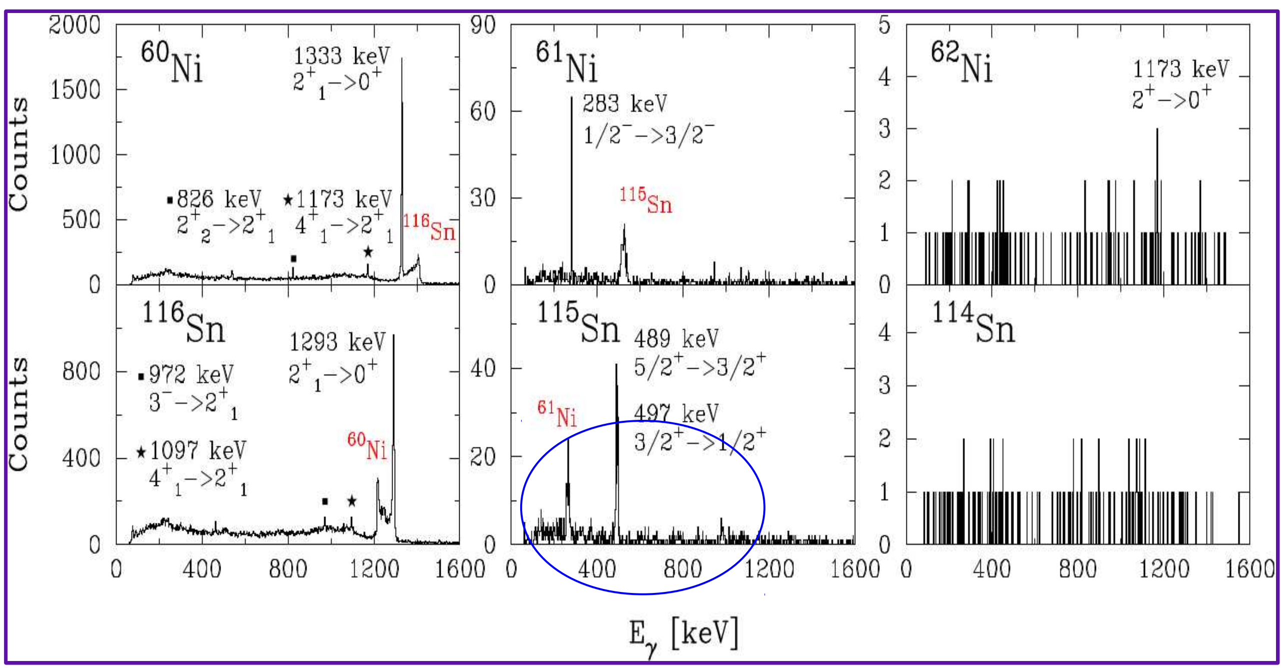

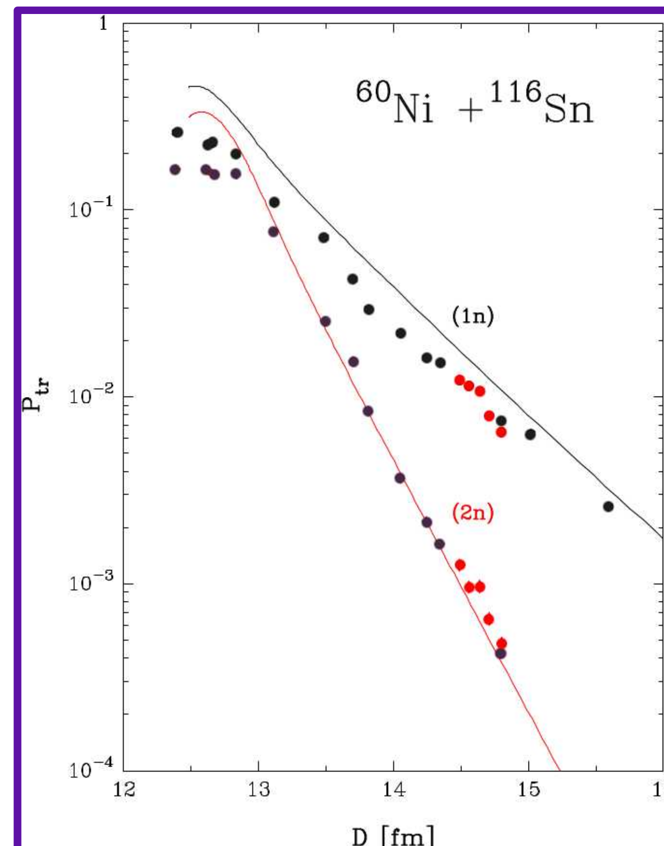

^{60}Ni+^{116}Sn, ^{40}Ca+^{96}Zr, ^{54}Fe+^{92}Mo: fragment – gamma measurements (PRISMA+CLARA/AGATA/LaBr)

The strengths (normalized to $2^+ \rightarrow 0^+$ in ^{60}Ni) of the most important transitions, corrected for the contributions of the feeding and for their relative detection efficiency in AGATA.
The direct population of states can be compared with any reaction code (DWBA, coupled channels, tabulated deformations, spectroscopic factors) → a direct check on the one-particle form factors (1n), and of the potential
(2n): no gamma in ^{114}Sn, few gamma in ^{62}Ni compatibile with $2^+ \rightarrow 0^+$ transitions →
$\sigma_{g.s} = \sigma_{tot} - \sigma_{exc}$ → **the transitions to the excited states contribute to the total strength: <24%, dominant population of the ground states**

	Experiment	Theory
^{116}Sn(2^+)	0.792 ± 0.160	0.720
^{116}Sn(4_1^+)	0.042 ± 0.011	0.056
^{60}Ni(4_1^+)	0.060 ± 0.013	0.11
^{115}Sn($5/2^+$)	0.018 ± 0.003	0.037
^{61}Ni($1/2^-$)	0.014 ± 0.003	0.033
^{62}Ni(2^+)	< 0.00145	-

E_γ [keV]

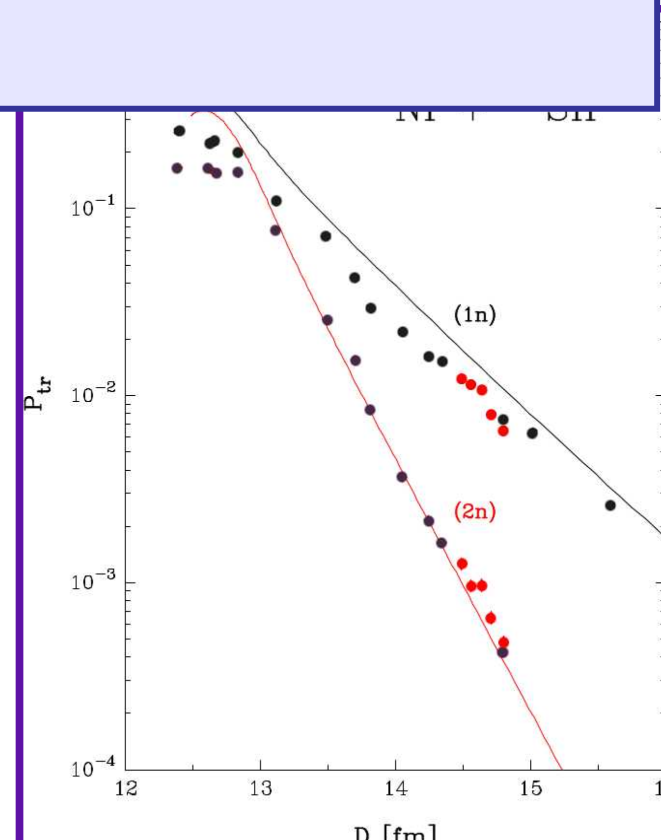

^{116}Sn+^{60}Ni: two particle transfer (semiclassical theory, microscopic calculations, 2nd order Born app.)

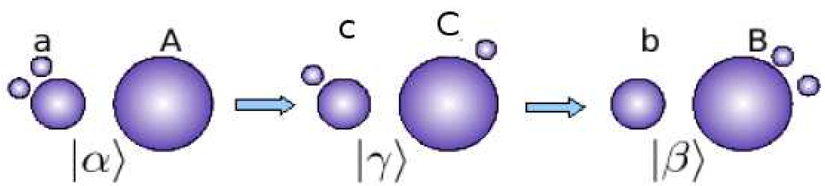

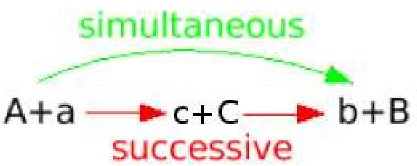

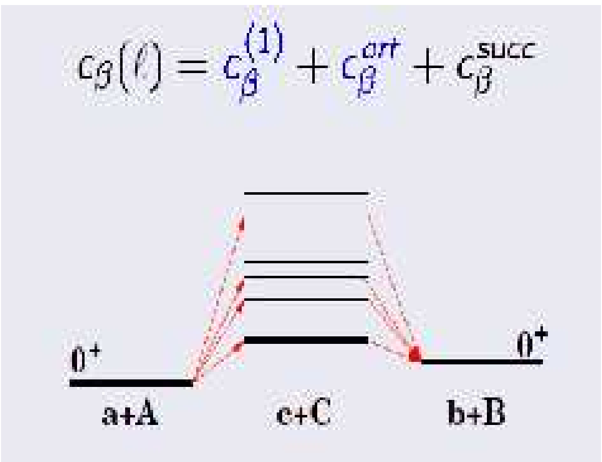

	nlj
^{116}Sn	$1g_{9/2}$
	$2d_{5/2}$
	$1g_{7/2}$
	$3s_{1/2}$
	$2d_{3/2}$
	$1h_{11/2}$
	$2f_{7/2}$
	$3p_{3/2}$
^{60}Ni	$2p_{3/2}$
	$2p_{1/2}$
	$1f_{5/2}$
	$1g_{9/2}$

3 terms : simultaneous, orthogonal and successive

only the successive term contributes to the transfer amplitude (simultaneous component is canceled out by the nonorthogonality correction)

Only 0+ to 0+ transitions are included (BCS).

$$(c_\beta)_{\rm succ} = \frac{1}{\hbar^2}\sum_{a_1,a_1'} B^{(A)}(a_1 a_1;0) B^{(a)}(a_1' a_1';0) 2\frac{(-1)^{j_1+j_1'}}{\sqrt{(2j_1+1)}\sqrt{(2j_1'+1)}}\sum_{m_1 m_1'}(-1)^{m_1+m_1'}$$
$$\times \int_{-\infty}^{+\infty} dt\, f_{m_1 m_1'}(\mathcal{R}) e^{i[(E_\beta - E_\gamma)t + \delta_{\beta\gamma}(t) + \hbar(m_1' - m_1)\Phi(t)]/\hbar}$$
$$\times \int_{-\infty}^{t} dt\, f_{-m_1 - m_1'}(\mathcal{R}) e^{i[(E_\gamma - E_\alpha)t + \delta_{\gamma\alpha}(t) - \hbar(m_1' - m_1)\Phi(t)]/\hbar}.$$

^{60}Ni+^{116}Sn: neutron pair transfer far below the Coulomb barrier

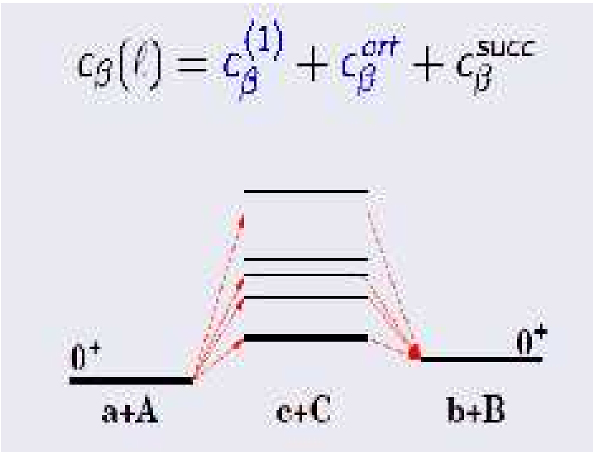

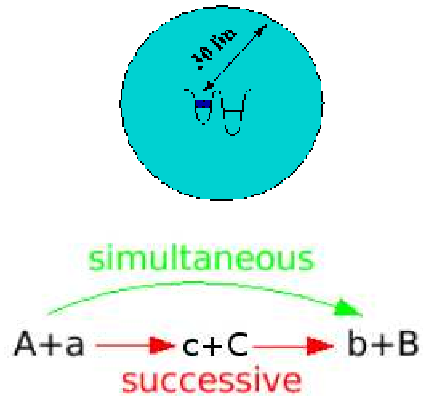

The experimental transfer probabilities are well reproduced, in absolute values and in slope by microscopic calculations which incorporate nucleon-nucleon correlations:

✓ a consistent description of (1n) and (2n) channels

✓ the formalism for (2n) incorporates the contribution from both the simultaneous and successive terms (only the ground-to-ground-state transition has been calculated)

✓character of pairing correlations manifests itself equally well in simultaneous and in successive transfers due to the correlation length

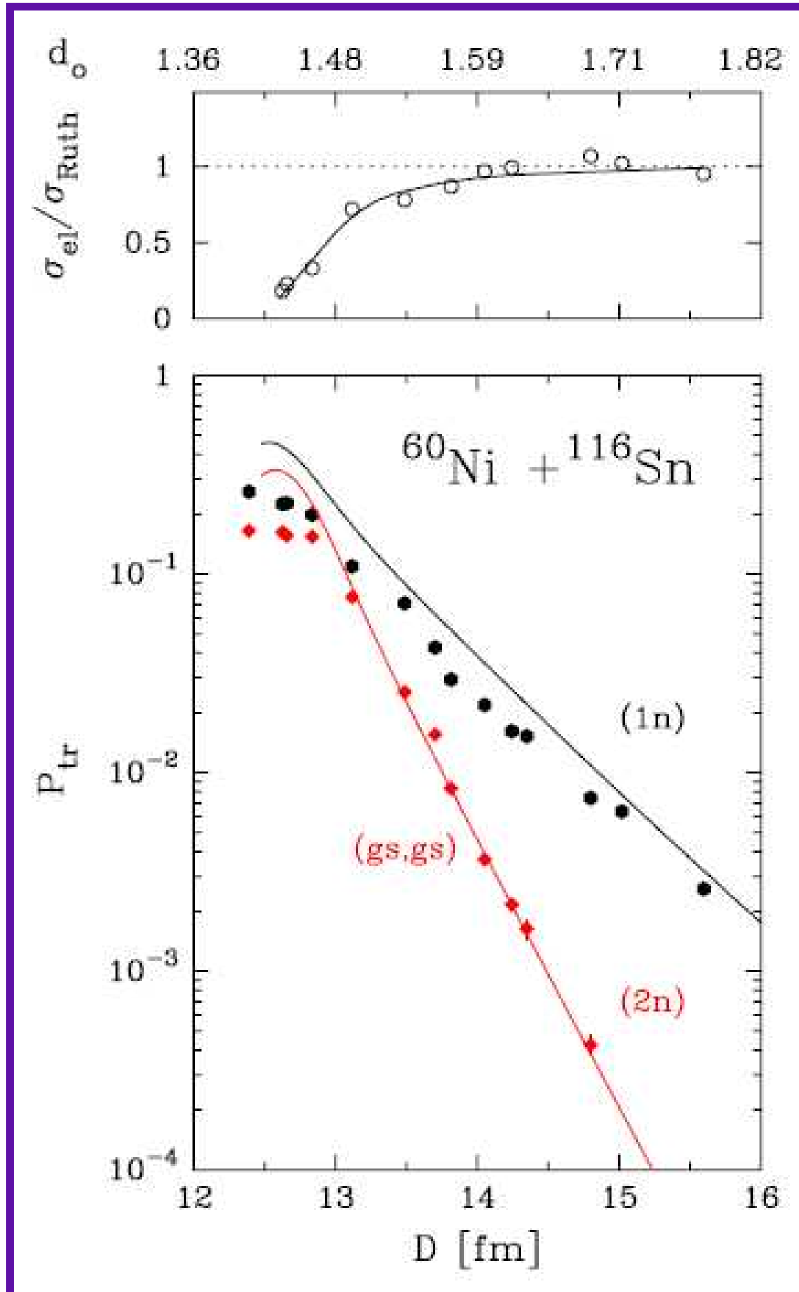

Sub-barrier transfer : TDHF or TDHF+BCS

$^{40}Ca+^{96}Zr$

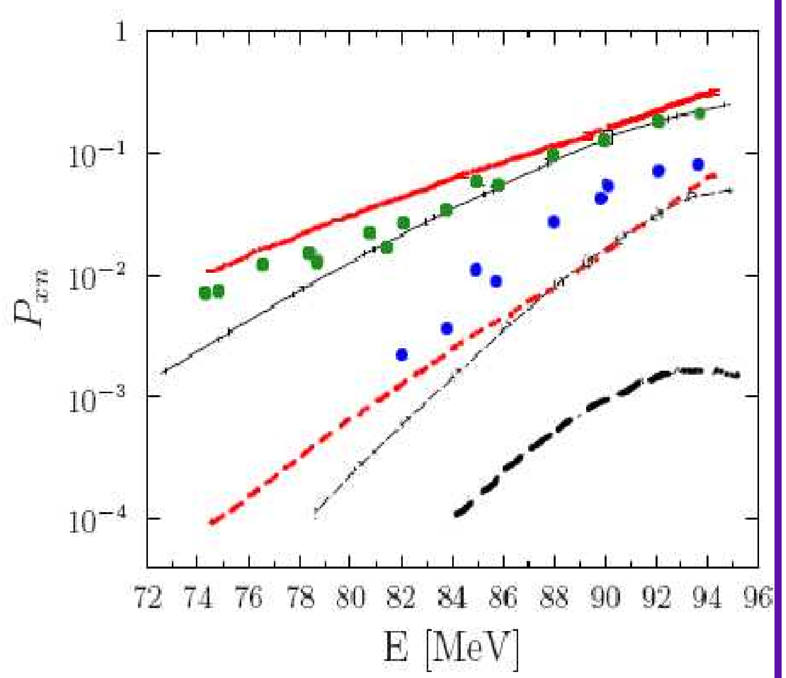

______(2n) TDHF+BCS
- - - - - -(1n) TDHF+BCS

EXP (1n) and (2n);
(1n) c.c.; (2n) (g.s. →g.s.)
(g.s. → 0+ at ~6MeV)

G.Scamps et al., EPJ Web Conf. 86 (2015) 00042

$^{16}O+^{208}Pb$

______(2n) TDHF
- - - - - -(1n) TDHF

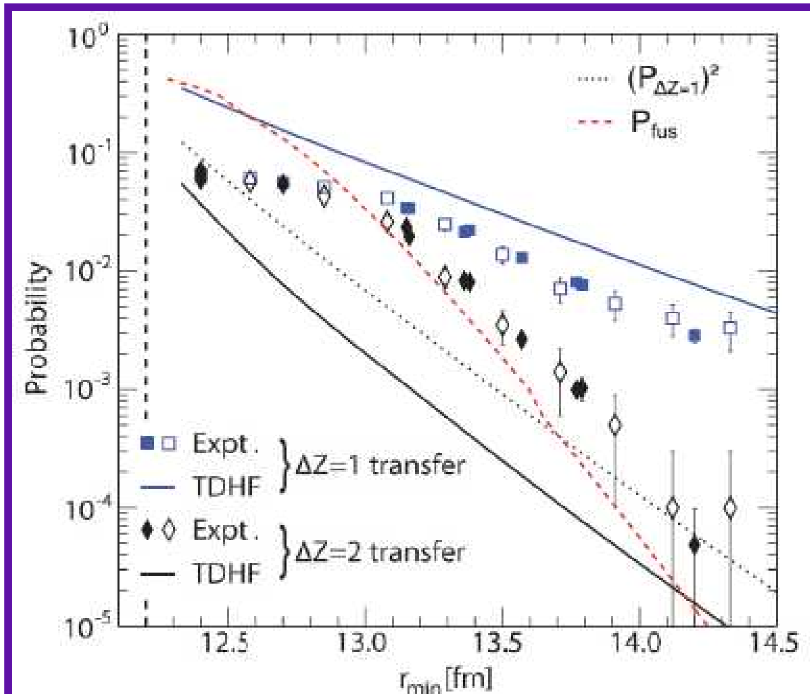

C.Simenel, PRL105(2010)192701

M.Evers et al, PRC84(2011)054614

Probing correlations in very-heavy systems: ^{206}Pb+ ^{118}Sn

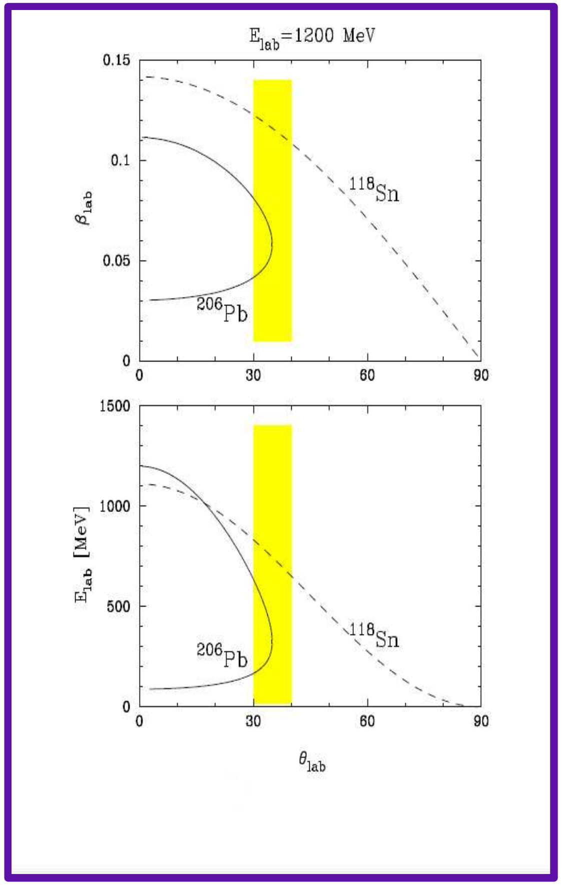

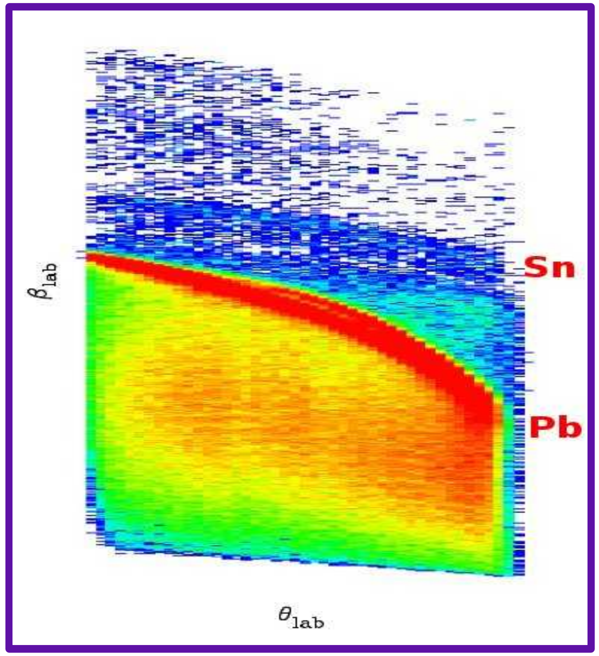

θ_{lab}=35^o is close to the limiting angle for Pb-like ions, so one can safely control the correct geometry of the experiment

at θ_{lab}=35^o Sn-like ions have kinetic energies ~ 750 MeV at E_{lab}=1200 MeV, so one expects good A and Z resolutions

➔ whether and to what extent **the effect of neutron-neutron correlations** in the evolution of the reaction is modified in the presence of **high Coulomb fields.**
➔ in the collision between **very heavy ions,** population of final states with high excitation and angular momenta may significantly change the transfer strength for the g.s. to g.s. transitions.

Energy spectra of $^{206}Pb+^{118}Sn$: complex reaction mechanism

E(^{206}Pb)=950 MeV

$\theta_{lab}=35^o$

ΔE

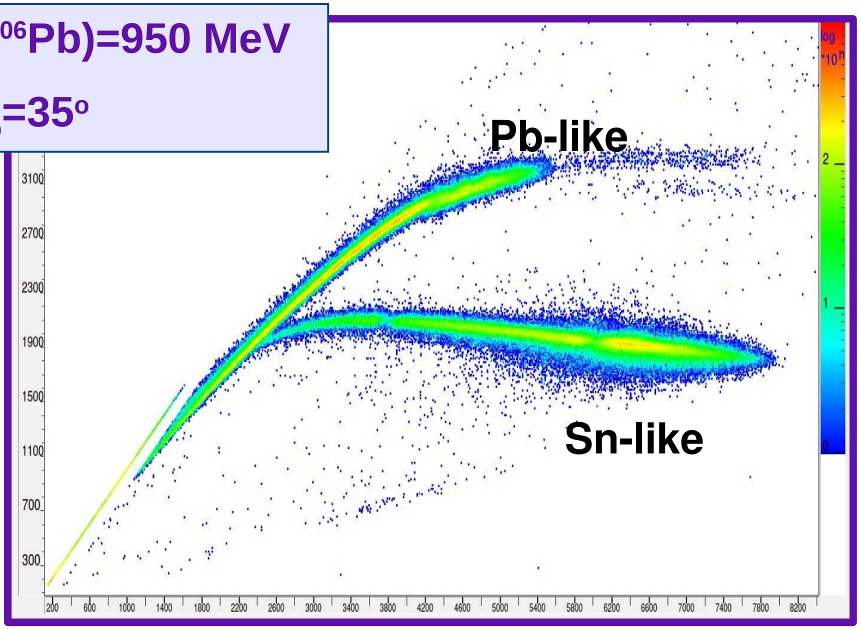

E(^{206}Pb)=1200 MeV

$\theta_{lab}=25^o$

ΔE

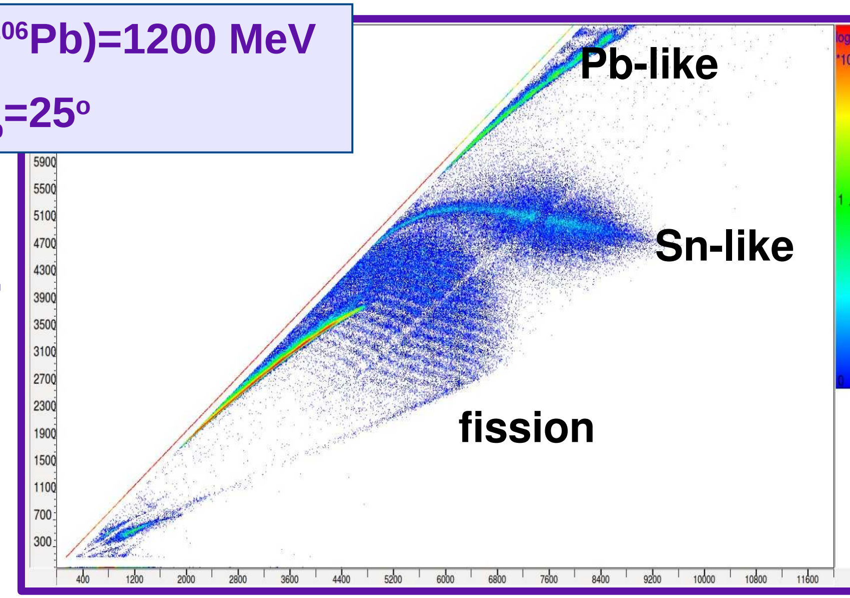

E

The yields of QE and DIC components (and fission fragments) strongly depend on (both) bombarding energy and angles

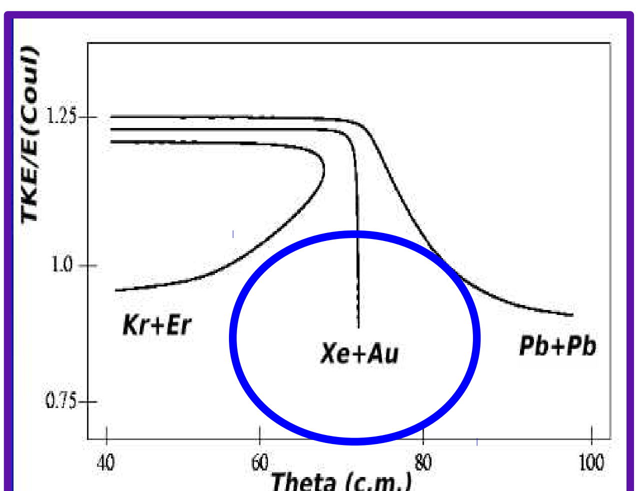

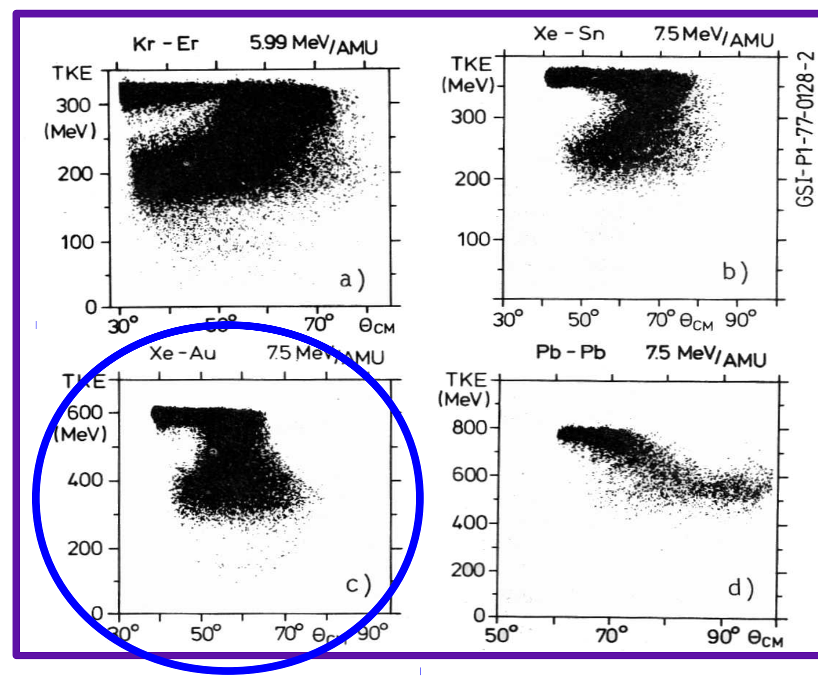

Nucleon transfer: exp. vs microscopic calculatons

^{96}Zr+^{40}Ca ("closed shell")

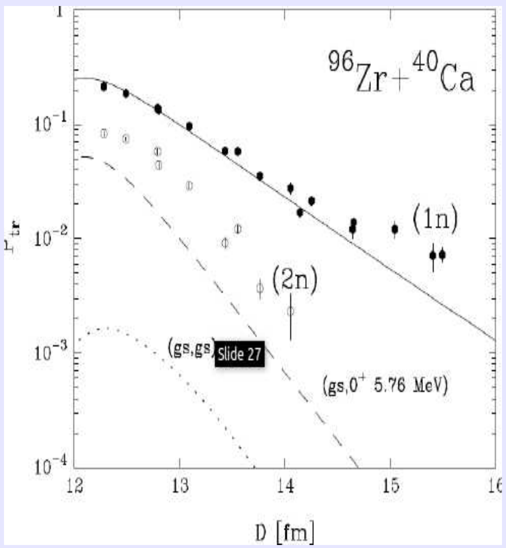

^{116}Sn+^{60}Ni ("superfluid")

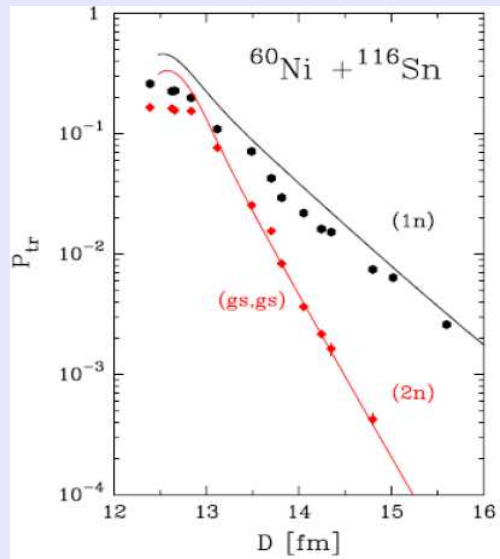

^{206}Pb+^{118}Sn ("heavy")

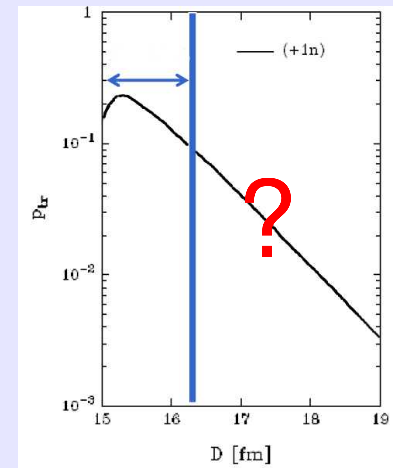

^{132}Sn+^{40}Ca,^{64}Ni,^{208}Pb ("neutron rich")

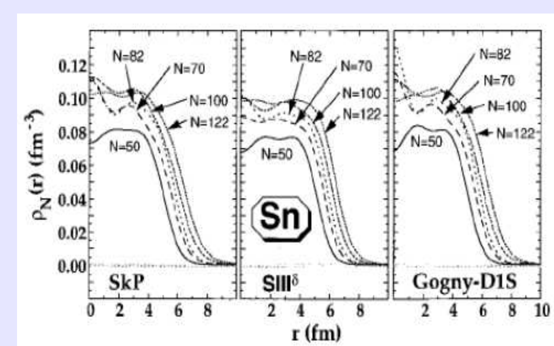

informations about correlations are extracted when experimental absolute cross sections are compared with a microscopic theory which beside correlations includes also the coupling between relative motion (reaction) and intrinsic motion (structure).

The synthesis of heavy nuclei

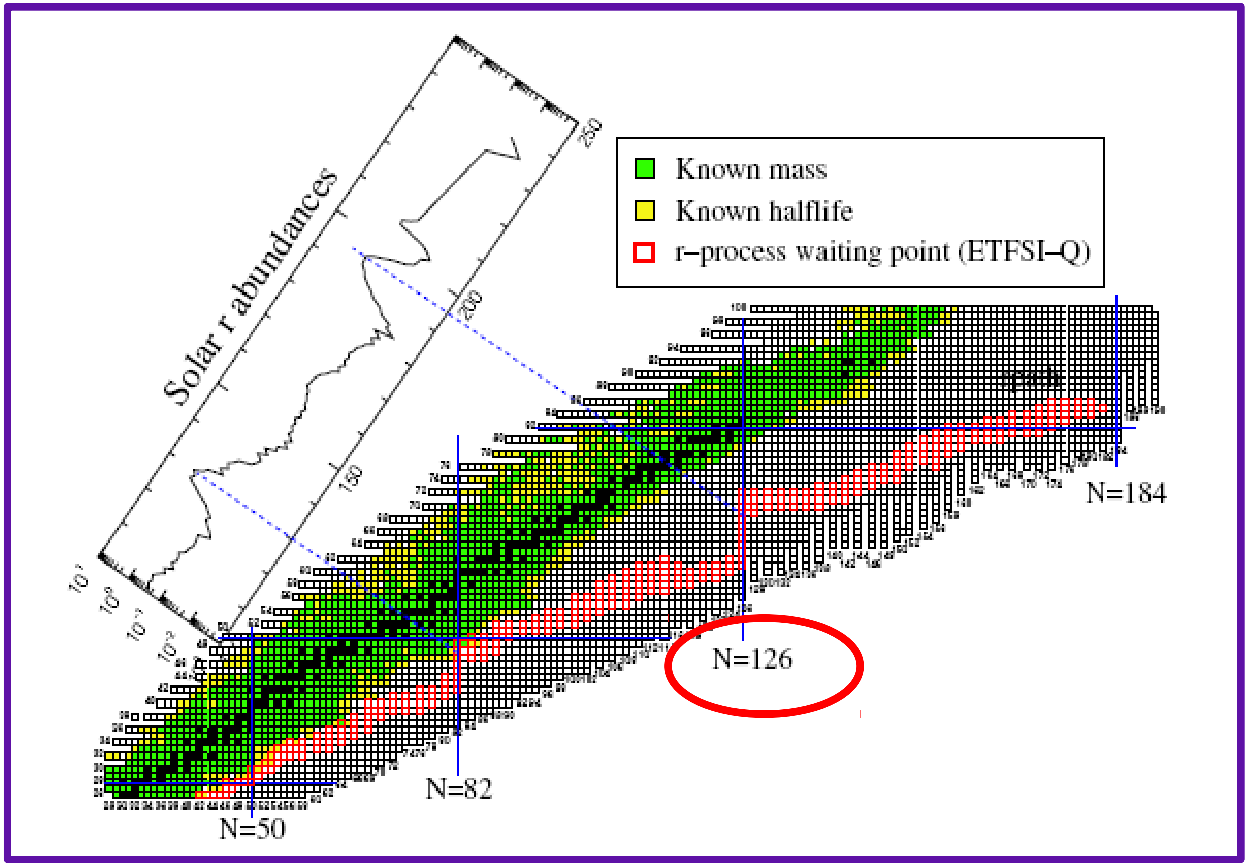

- HOW: rapid neutron capture
- WHERE: neutron stars merger

"The transients, named 'macronovae' or 'kilonovae', are believed to be cradles of production of rare elements such as gold and platinum."

- Important to know masses, structure, life times, decay modes
- Very important to know these characteristic close to the neutron magic numbers N = 50, 82, 126 (define the r-process path and strong peaks in Solar system abundances)

Luminosity depends on the transparency of the ejecta, even a very small amount of heavy elements and nuclei can strongly modify the spectral distributions and observations.

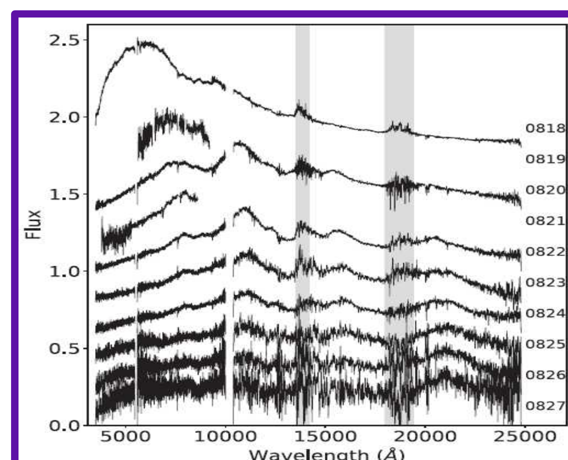

H. Grawe et al, Rep. Prog. Phys. 70 (2007) 1525.
D. Kasen et al., Nature 551 (2017) 80; E. Pian et al., Nature 551 (2017) 67.

Synthesis of heavy neutron rich nuclei in labs

Fusion by using neutron-rich radioactive beams $\rightarrow$ the intensity of the beams rather small (accelerators)

Neutron capture reaction $\rightarrow$ the intensity of the neutron beams is small (reactors)

relativistic energies : fragmentation reactions
energies close to the Coulomb barrier : multinucleon transfer reactions
$\rightarrow$ cross sections ~ μb – nb
$\rightarrow$ detection systems: large solid angle, large efficiency, large selectivity...

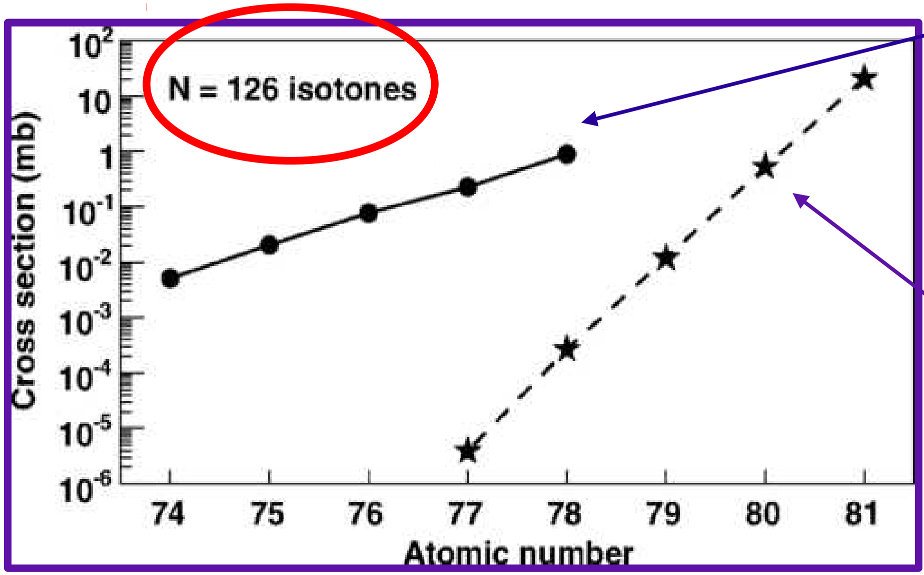

multinucleon transfer reactions:
$^{136}Xe + ^{198}Pt$ @ E_{lab}= 8 MeV/A

fragmentation reactions:
$^{208}Pb + ^{9}Be$ @ E_{lab}= 1 GeV/A

Y. Watanabe et al, Phys. Rev. Lett. 115 (2015) 172503, T. Kurtukian-Nieto et al., Phys. Rev. C 89 (2014) 024616.

Multinucleon transfer reactions

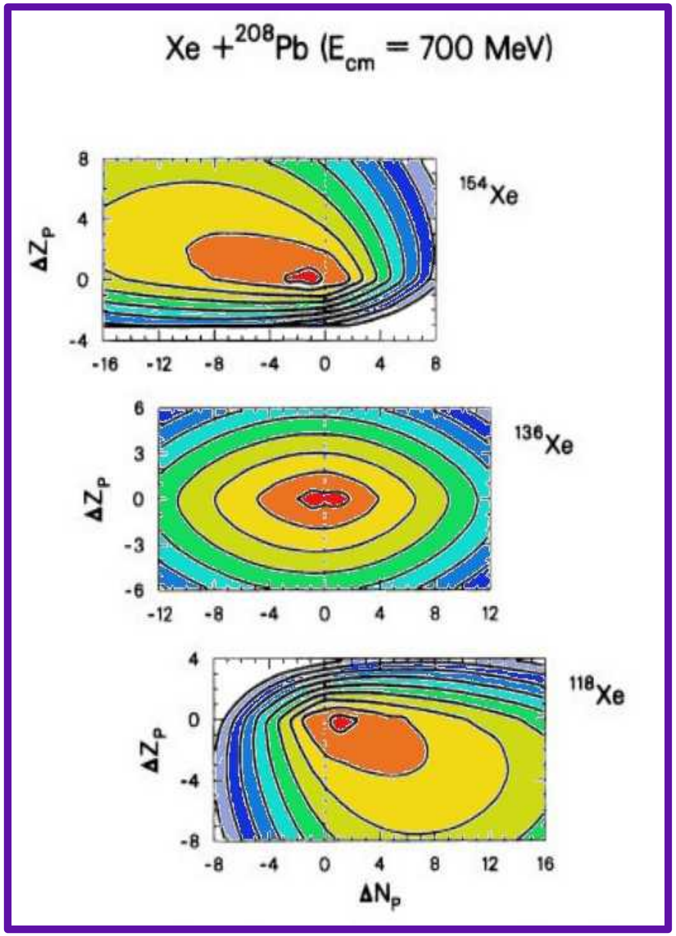

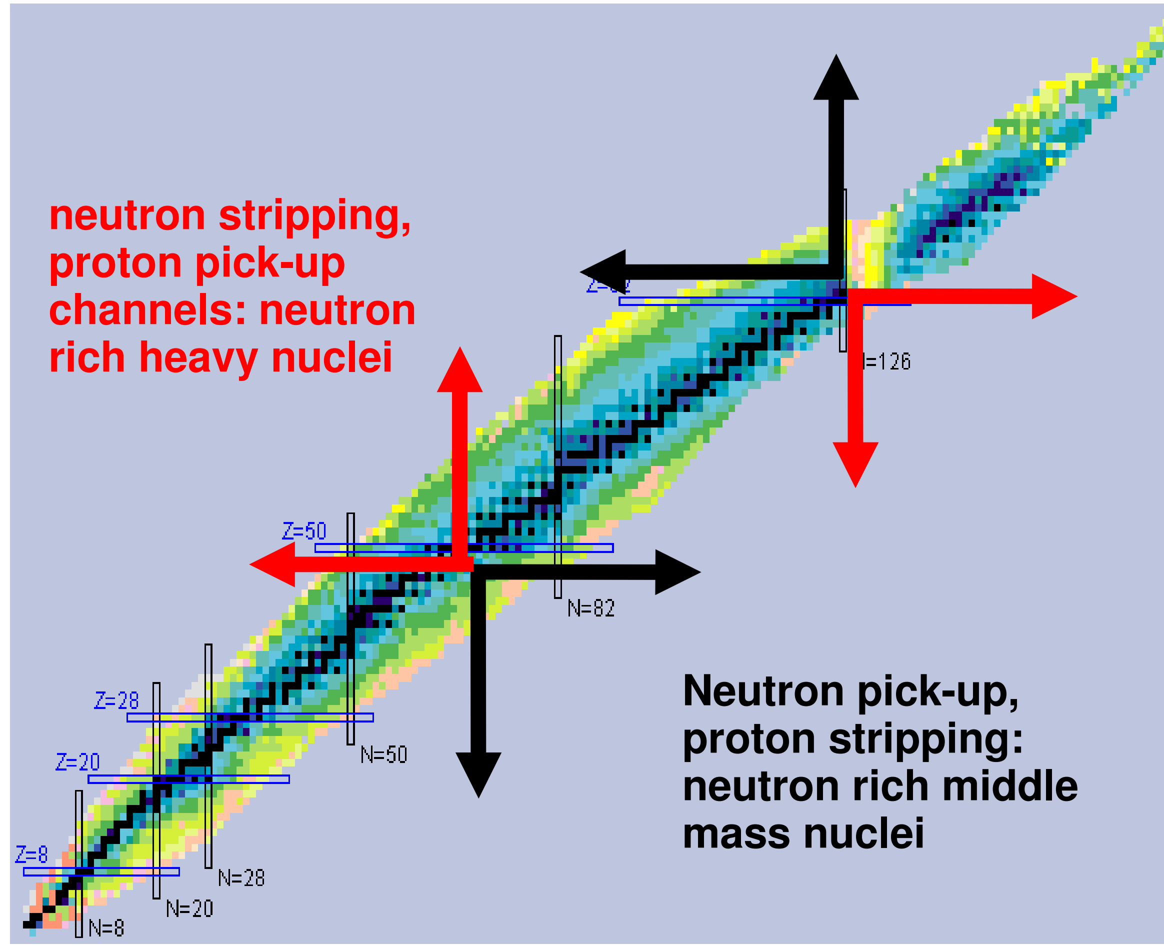

Xe (Z=54)
^{118}Xe ($T_{1/2}$ = 4 min)
^{136}Xe ("the last" stable)
^{154}Xe (no information)

TH: C.H. Dasso, G. Pollarolo and A. Winther, Phys. Rev. Lett. 73 (1994) 1907.
EXP: L. Corradi, G. Pollarolo, S. Szilner, J. Phys. G 36 (2009) 113101 (Special Topic)

$^{40}Ar+^{208}Pb$

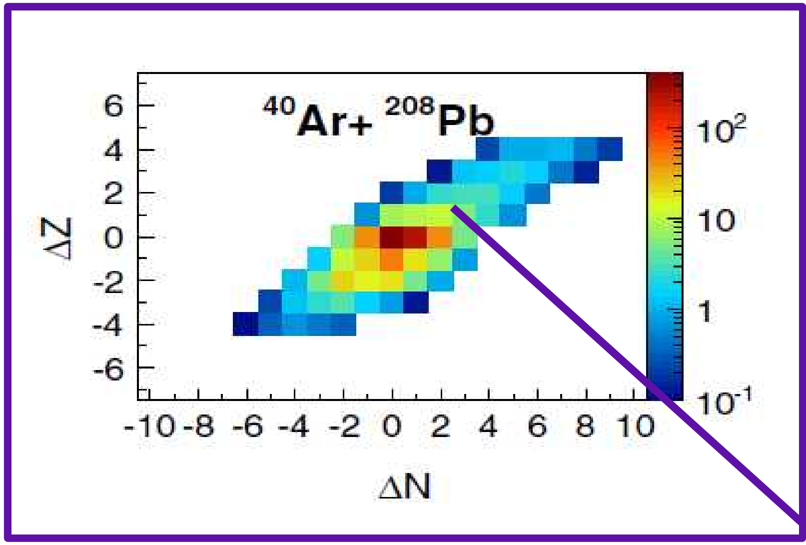

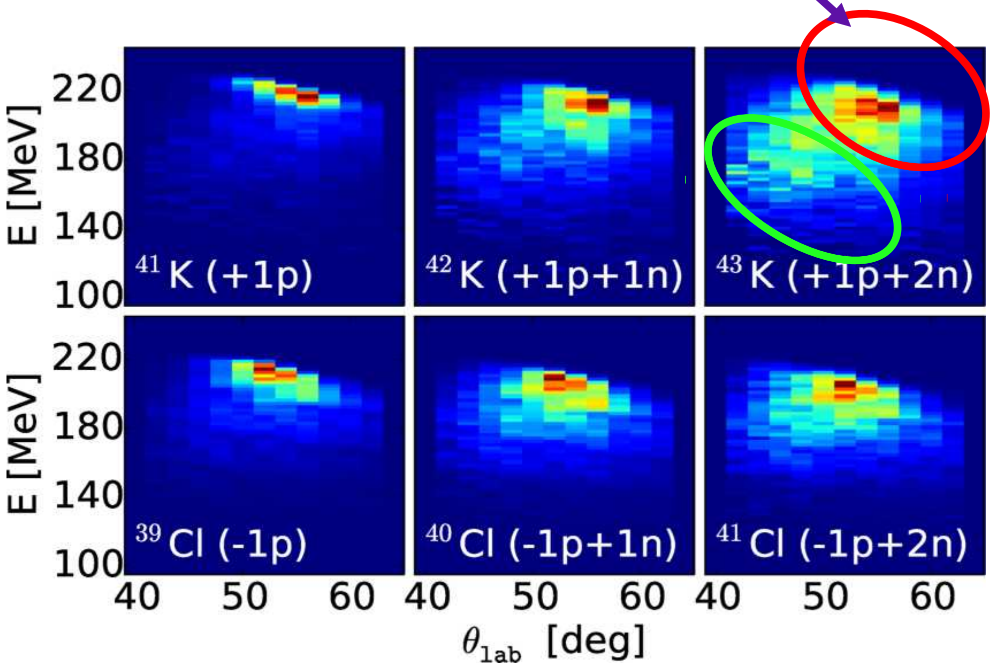

Wilczynski plots

- ✓Reaction develops from quasi-elastic to deep inelastic
- ✓Secondary processes are important – survival probability of the heavy binary partner

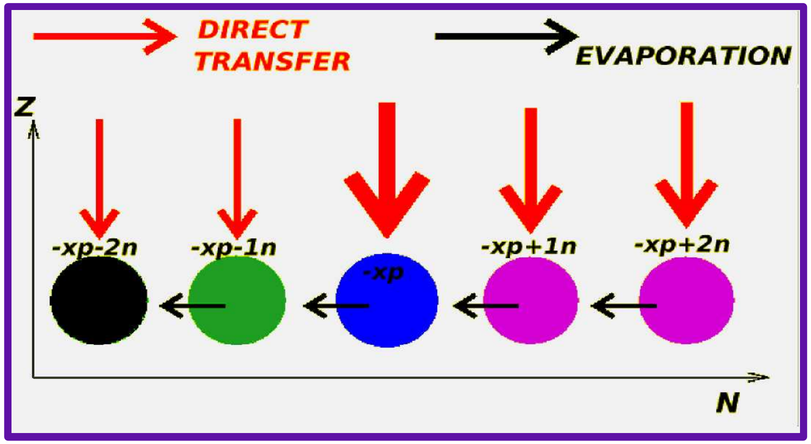

Secondary processes: fission, evaporation of neutrons may strongly modify the final cross sections

T. Mijatović et al., Phys. Rev. C 94 (2016) 064616

Mass correlation between light and heavy reaction products in multinucleon transfer $^{197}Au+^{130}Te$ collisions

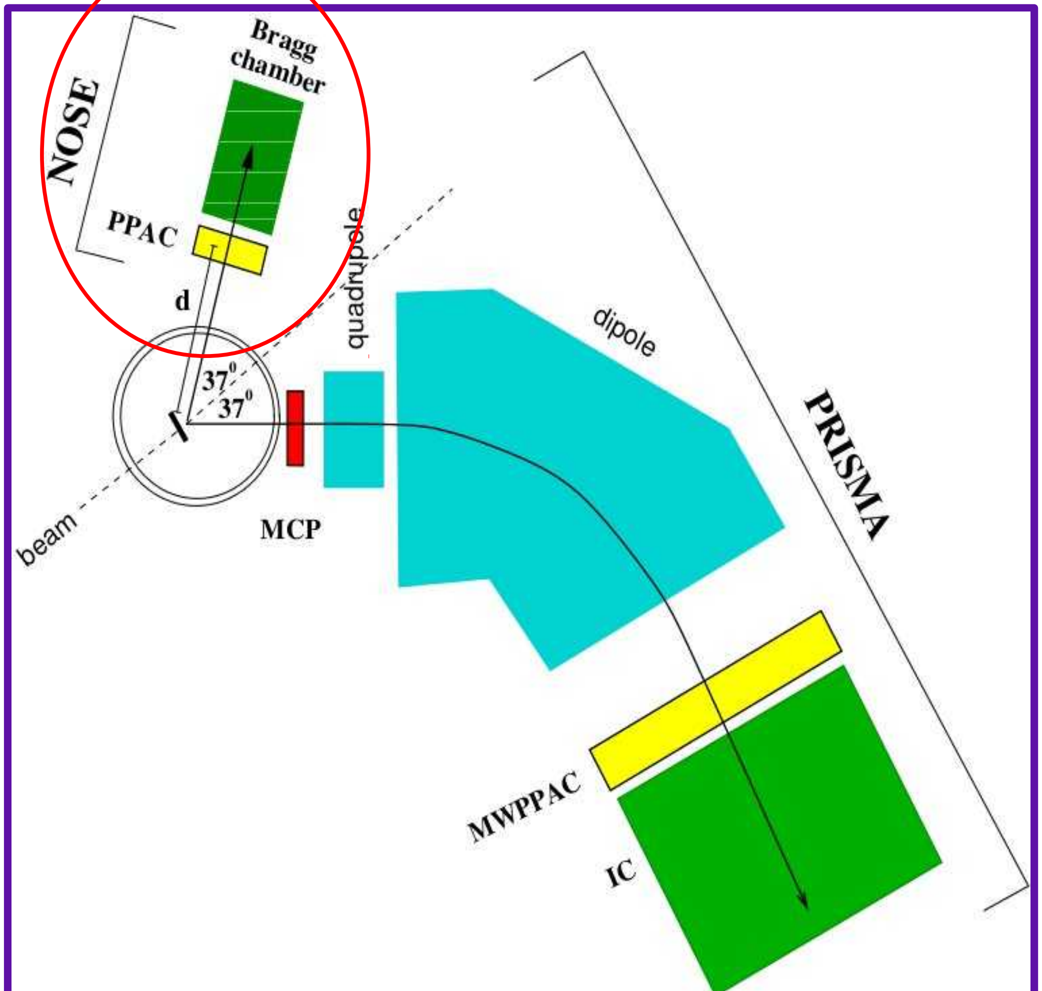

Coincident detection of binary partners: PRISMA (Te-like) + NOSE (Au-like)
NOSE: (solid angle ~1/3 PRISMA solid angle): PPAC (multiwire parallel-plate avalanche counter) + ionization chamber (an axial-field ionization chamber, Bragg chamber)
→ time signal, 2-dim position signal (the time and position resolution similar as in PRISMA, ~1mm, ~350ps)
→ identification through the Bragg peak, total energy, and range

A gas detection system for fragment identification in low-energy heavy-ion collisions
E. Fioretto et al. Nucl. Inst. and Meth. A 899 (2018) 73

$^{197}Au+^{130}Te$: coincident detection of binary partners

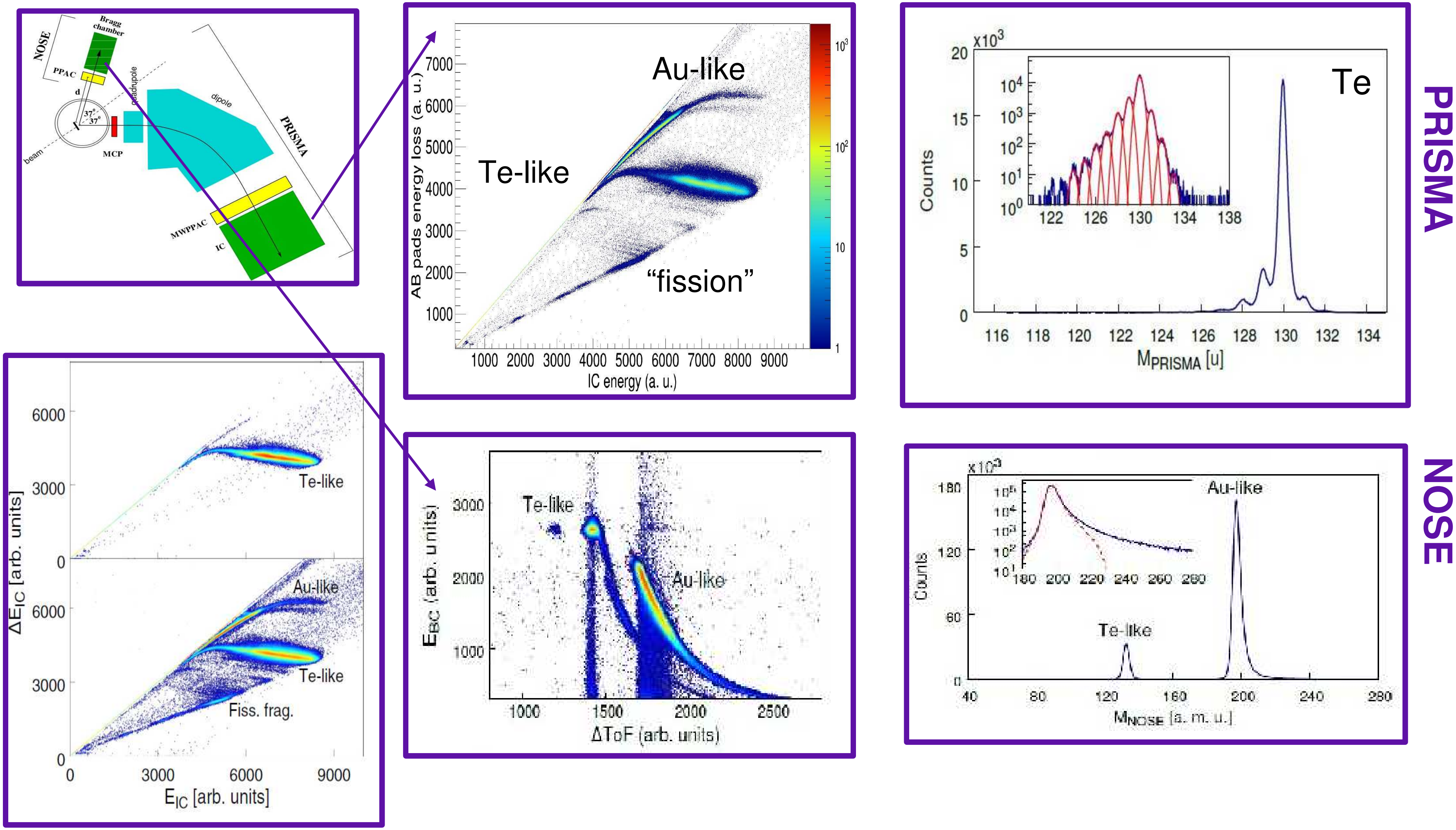

F. Galtarossa et al., Phys. Rev. C 97 (2018) 054606

$^{197}Au+^{130}Te$

^{197}Au+^{130}Te: coincident detection of binary partenrs

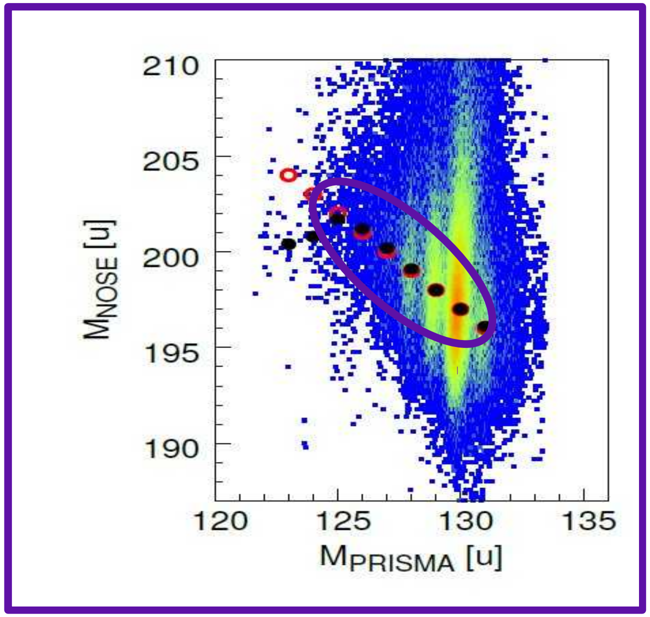

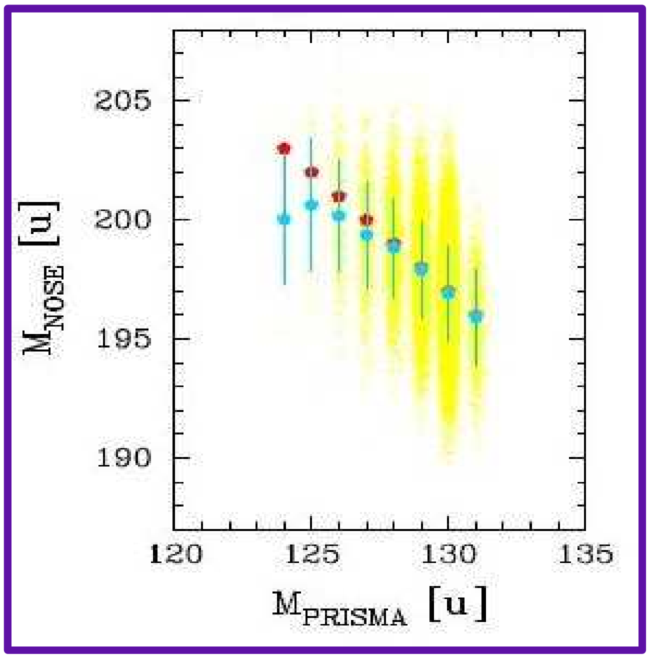

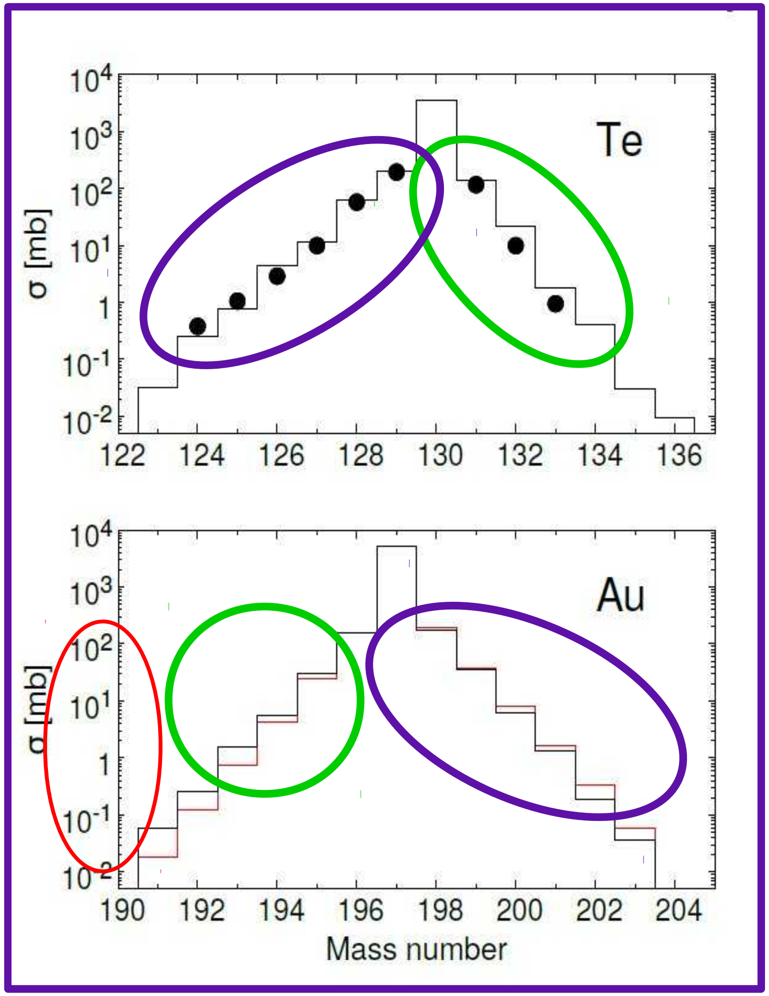

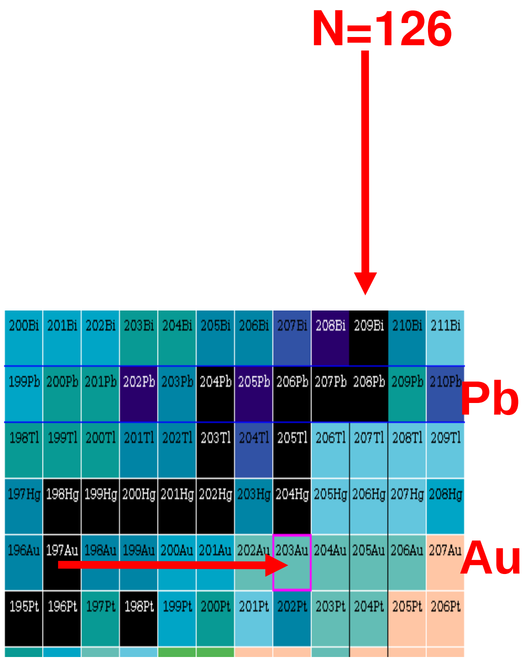

Multinucleon transfer reactions are suitable tool for the production of the heavy neutron-rich nuclei

Te isotopes with “more” neutrons than in ^{130}Te

Au isotopes with “more” neutrons than in ^{197}Au

^{94}Rb+^{208}Pb: MNT with neutron-rich beam

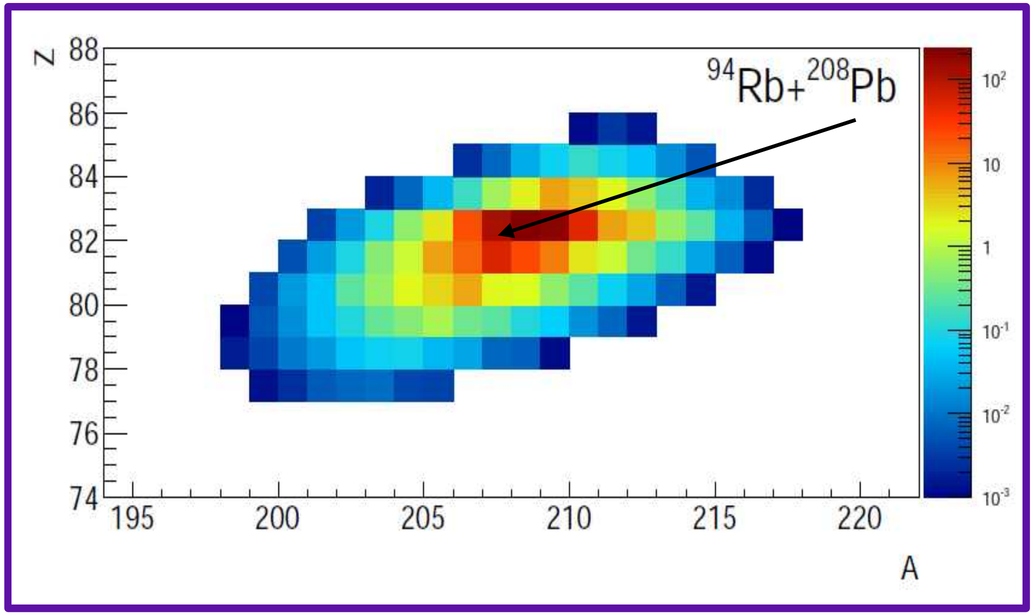

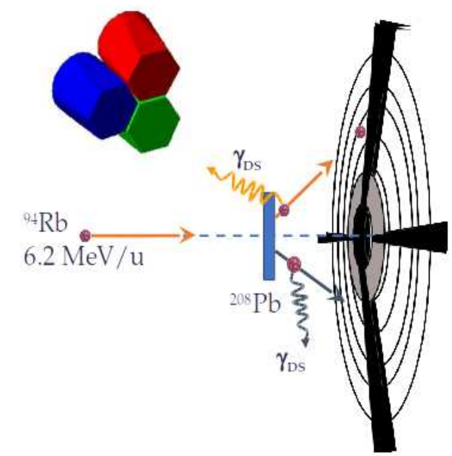

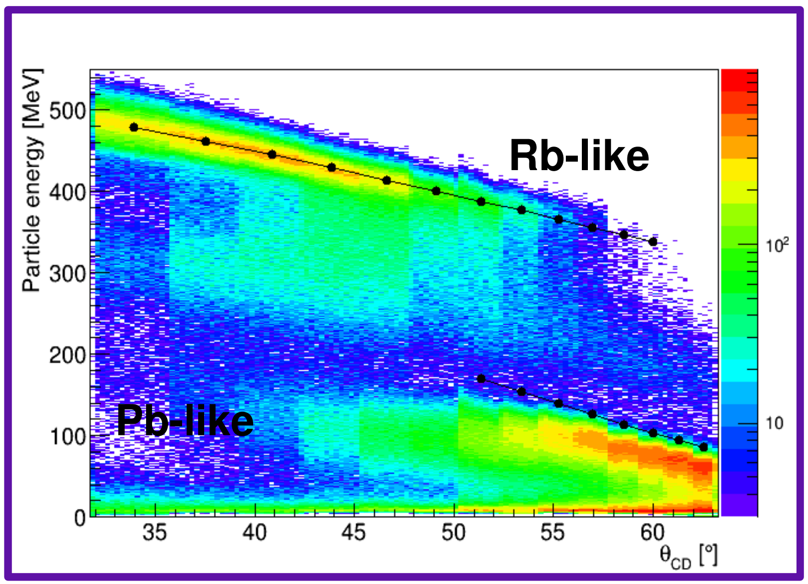

ISOLDE – CERN: MINIBALL + CD particle detector → fragment-gamma(-gamma) coincidencies

→ preliminary results: dominant cross sections in the “south-west” region

P. Čolović poster 151
Study of the neutron-rich region in the vicinity of ^{208}Pb via multinucleon transfer reactions

ISOLDE EXP IS572, spokespersons:
J.J. Valiente Dobon and S. Szilner

Summary and outlook

MNT reaction around the Columomb barrier → suitable tool to study

nucleon-nucleon correlations
→ “large” spectrometers coupled to “large” gamma arrays are powerful tools to study the correlations
→ sub-barrier transfer reaction measurement (nuclei interact at large distances): good probe for pair correlations
→ The information about correlations are extracted when experimental **absolute** cross sections are compared with a microscopic theory which beside correlations includes also the coupling between relative motion (reaction) and intrinsic motion (structure).
→ further developments of microscopic models needed (proton channels)

production of heavy neutron-rich nuclei
→ PRISMA – detection of heavy low-energy ions
→ The comparison between data and theory: elementary modes of the complex mechanism can be probed.
→ new perspective: the use of (very) neutron-rich projectiles (RIB)
→ more exp. studies of the best selection of mass asymmetry and collision energy for the largest survival probabilities of heavy partners
→ further development of the instrumentation for coincidence detection of both partners (see next talk: **KEK isotope separation system, Yutaka Watanabe)**

L. Corradi, G. Pollarolo, T. Mijatović, F. Galtarossa, P. Čolović, A. Goasduff, D. Montanari, E. Fioretto, A.M. Stefanini, G. Montagnoli, G. Colucci, F. Scarlassara, J.J. Valiente-Dobon, D. Mengoni, D. Jelavić Malenica, N. Soić, N. Vukman, M. Milin, D. Nurkić and CLARA-AGATA collaboration

Ruđer Bošković Institute, Zagreb, Croatia
INFN - Laboratori Nazionali di Legnaro, Legnaro, Italy
INFN and Universita di Torino, Italy
INFN and Universita di Padova, Padova, Italy
University of Zagreb, Croatia

Kokopelli: links distant and diverse communities together.

This work was partly supported by the Croatian Science Foundation under the project 7194 and IP-2018-01-1257.

NOSE – an ancillary detector coupled to PRISMA

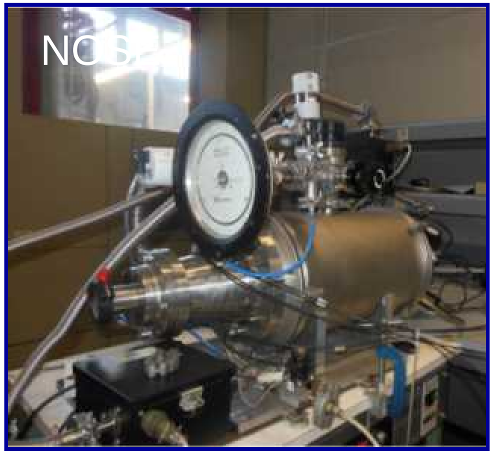

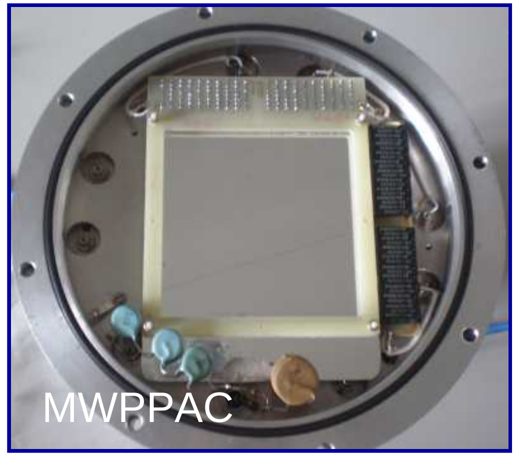

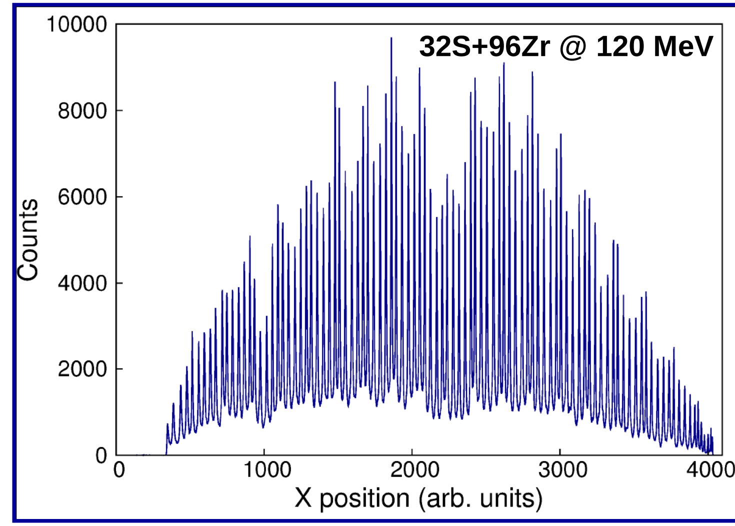

Bragg Curve Spectroscopy

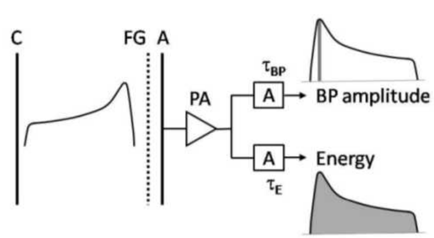

E. Fioretto et al., NIM A 899 (2018) 73

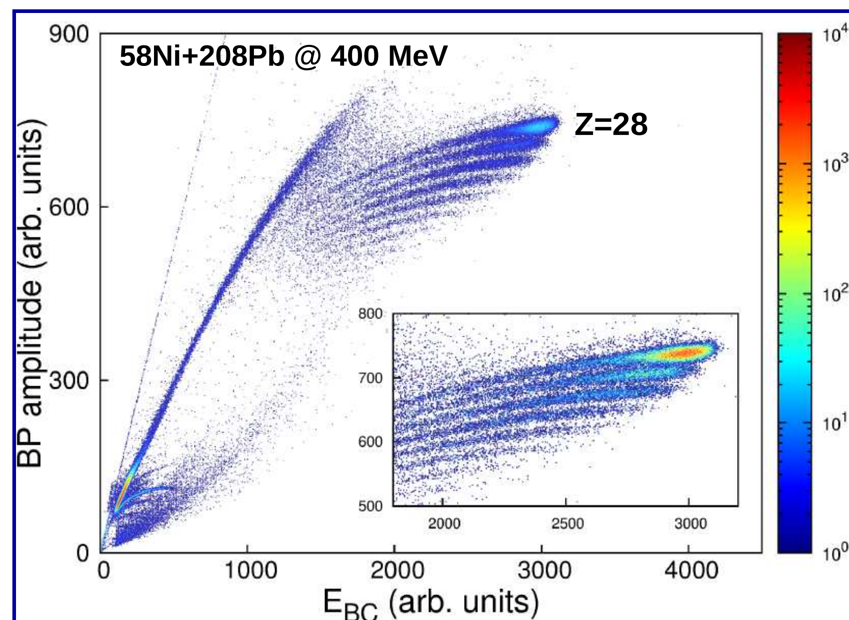

$\Delta Z/Z$ ~ 1/60

NOSE – an ancillary detector coupled to PRISMA

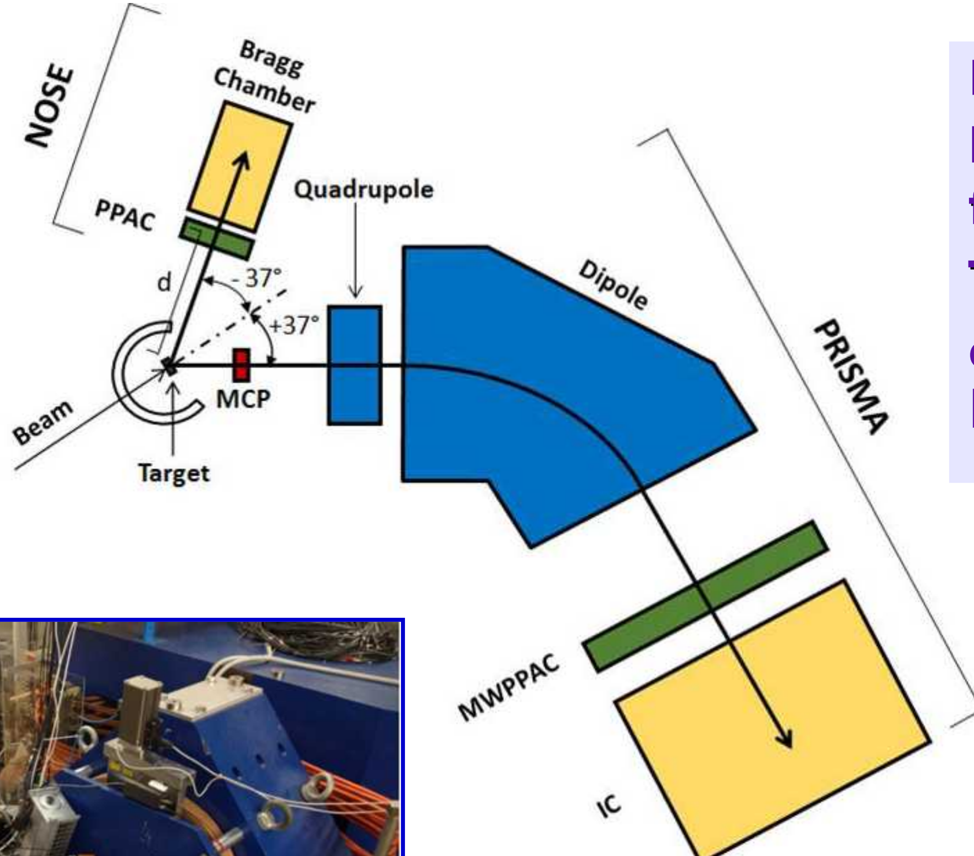

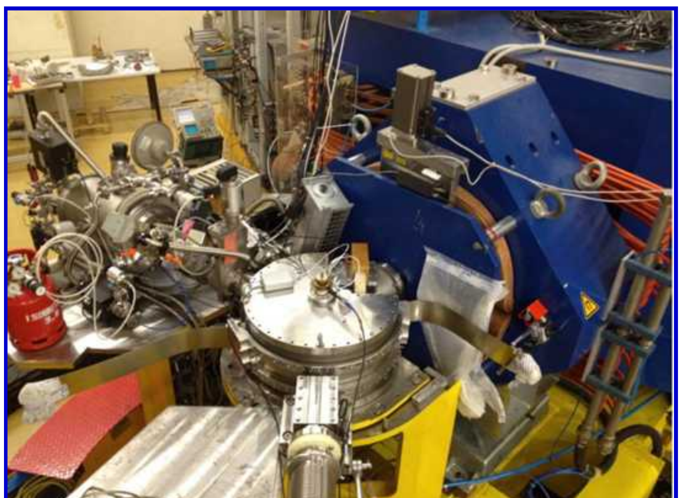

PRISMA:
position in MCP: X_i, Y_i
focal plane position: x_f, y_f
Time of Flight: $ToF = t_f - t_i$
energy loss, total energy: ΔE, E - IC

PRISMA: ΔA/A ~ 1/250
NOSE: ΔA/A ~ 1/40

NOSE:
position in PPAC: X_N, Y_N
Time of Flight: $ToF = t_i - t_N$
(MCP_{PRISMA} - $PPAC_{NOSE}$)
BC: E, Z